A global view of isotopic effects on ro-vibrational spectra of six-atomic molecules: a case study of eleven ethylene species

Dominika Viglaska-Aflalo, Michael M. Rey, Andrei Nikitin, Thibault Delahaye

Global view on isotopic effects in ro-vibrational spectra of six-atomic molecules: case study of eleven ethylene species

Dominika Viglaska-Aflalo,*[a] Michaël Rey,[a] Andrei Nikitin,[b,c] and Thibault Delahaye[d]

In this work, we present a global view of the impact of isotopic substitutions on eleven ethylene isotopologues spectra obtained from variational calculations using accurate *ab initio* potential energy and dipole moment surfaces. That may lead to some important changes in molecular spectra due to symmetry breaking effects lowering the initial D_{2h} symmetry of $^{12}C_2H_4$ ($\equiv$ $^{12}CH_2{}^{12}CH_2$) to C_{2v}, C_{2h} or C_s. For the very first time, we report *ab initio* predictions for $^{12}C_2D_4$ ($\equiv$ $^{12}CD_2{}^{12}CD_2$) and three C_s species : $^{12}CHD^{13}CH_2$, $^{13}CHD^{12}CH_2$ and $^{12}C_2HD_3$ ($\equiv$ $^{12}CD_2{}^{12}CHD$). To this end, we have considered the normal-mode approach based on our reduced Eckart-Watson Hamiltonian combined with ethylene *ab initio* surfaces. This work will contribute to the complete theoretical studies of the deuterated and ^{13}C-enriched ethylene isotopologues. A total of 1252 vibrational levels is computed and all the corresponding transitions in the energy range ≤ 3100 cm^{-1} are predicted and compared to 151 bands assigned from experimental spectra analyses.

[a] *Groupe de Spectrométrie Moléculaire et Atmosphérique, UMR CNRS 7331, BP 1039, F-51687, Reims Cedex 2, France; E-mail: dominika.viglaska@univ-reims.fr, michael.rey@univ-reims.fr*
[b] *Laboratory of Theoretical Spectroscopy, Institute of Atmospheric Optics, SB RAS, 634055 TOMSK, Russia.*
[c] *Laboratory of Quantum Mechanics of Molecules and Radiative Processes, Tomsk State University, 36 Lenin Avenue, 634050 Tomsk, Russia*
[d] *Laboratoire de Météorologie Dynamique/IPSL, CNRS, Ecole polytechnique, Université Paris-Saclay, Palaiseau, 91128, France*

1 Introduction

Isotopic substitution may considerably affect the molecular properties related to absorption or emission of radiation. In the Born-Oppenheimer approximation, an isotopic substitution does not alter the nuclear potential energy surface obtained by solving the electronic Schrödinger equation on a grid of nuclear geometries. Only the nuclear kinetic energy operator is changed. Because of symmetry breaking effects and different selection rules, some rovibrational structures in molecular spectra may also substantially change.

Hydrocarbon molecules are of particular importance due to their atmospheric, industrial, environmental and astrophysical applications [1–3]. Isotopically substituted molecules belonging to the family of small hydrocarbons were detected in several planetary atmospheres [4–13]. Note that the isotopologues considered for compounds in the terrestrial atmosphere [14] include D, T, ^{13}C and ^{14}C. Highly accurate and precise measurements of the isotopic composition of these molecules are now possible thanks to advances in mass and infrared spectrometry provided either by experiments on spatial missions or by laboratory measurements. These latters allow to determine accurately all isotopic ratios and are thus crucial for understanding the composition of different atmospheres (e.g. Earth, Venus, Mars, Jupiter, Saturn, Uranus, and Titan). Moreover, they provide precious information about the evolution of planets, their origin and the formation of our solar system [15,16]. For astrophysical applications, deuterated and ^{13}C enriched isotopologues are of particular importance because they allow to measure the D/H or ^{13}C/^{12}C ratio in the interstellar environment [17]. Consequently, its determination permits to explain the origin of several atmospheric compounds which themselves may play an important role in determining the overall thermal and chemical balance of the atmosphere [18,19]. The measurements of the observed fractionation issues from the chemical, physical and biological processes should be accomplished by theoretical, fundamental studies which will contribute to a better interpretation, analysis and understanding in a variety of environmental effects. Theoretical spectroscopy aims to provide accurate, reliable and complete theoretical line lists including a large amount of molecules studied over wide temperature and/or wavenumber ranges.

Ethylene possesses a rich variety of isotopologues (see Tab. 1 for different nomenclatures used in the literature). By

Table 1 Different nomenclatures used in the literature for ethylene isotopologues

Usual notation	Chemical formula
$^{12}C_2H_4$	$^{12}CH_2{}^{12}CH_2$
$^{12}C_2H_3D$	$^{12}CHD{}^{12}CH_2$
$cis-^{12}C_2H_2D_2$	$cis-^{12}CHD{}^{12}CHD$
$trans-^{12}C_2H_2D_2$	$trans-^{12}CHD{}^{12}CHD$
$as-^{12}C_2H_2D_2$	$^{12}CH_2{}^{12}CD_2$
$^{12}C_2HD_3$	$^{12}CD_2{}^{12}CHD$
$^{12}C_2D_4$	$^{12}CD_2{}^{12}CD_2$
$^{12}C^{13}CH_4$	$^{12}CH_2{}^{13}CH_2$
$^{13}C_2H_4$	$^{13}CH_2{}^{13}CH_2$
–	$^{12}CHD{}^{13}CH_2$
–	$^{13}CHD{}^{12}CH_2$

comparison with methane, the deuterated substitutions produce four species, namely CH_3D, CH_2D_2, CHD_3 and CD_4 belonging to three point groups [20–26] (T_d, C_{3v} and C_{2v}), while the $^{12}C \rightarrow {}^{13}C$ substitution does not change symmetry. In case of ethylene, both H $\rightarrow$ D and $^{12}C \rightarrow {}^{13}C$ substitutions produce a large variety of species that may lower symmetry and consequently strongly affect the overall molecular patterns.

The purpose of this paper is (*i*) to give an overview of the existing experimental and theoretical studies concerning ethylene isotopologues, (*ii*) to highlight the consequences of the H $\rightarrow$ D and/or $^{12}C \rightarrow {}^{13}C$ substitutions on the reorganization of the vibrational energy pattern and on the molecular spectra in ethylene molecule as well as (*iii*) to complete our previous studies [27,28] by providing first variationally predicted intensities for four additional ethylene isotopologues : $^{12}CHD{}^{13}CH_2$, $^{13}CHD{}^{12}CH_2$, $^{12}C_2D_4$ and $^{12}C_2HD_3$. By considering our previously reported studies, a total of 11 isotopic species belonging to D_{2h}, C_{2h}, C_{2v} and C_s symmetry groups is now available and freely accessible *via* the TheoReTS information system [29].

2 Overview of the isotopic dependence and spectral density of bands for ethylene isotopologues

The most extended theoretical spectra predictions for the main ethylene isotopologue $^{12}C_2H_4$ using molecular PES[30] and DMS[31] have been published in Ref.[32] (see also Ref.[33] as part of the Exomol project) and included in the TheoReTS information system[29]. A detailed overview of all existing experimental band centers and line position analyses for 8 isotopologues were provided in our previous works[27,28] where the corresponding line lists were provided. For $^{13}C_2H_4$, $^{13}C^{12}CH_4$, $^{12}C_2H_3D$ and for the three bi-deuterated *cis*, *trans*, *as*$-C_2H_2D_2$, rovibrational infrared spectra of these molecules were the subject of several investigations these past few decades both at low and high resolution. The Fourier transform infrared (FTIR) spectrometers permitted to record high-resolution spectra (with the uncertainty going up to 0.00096 cm^{-1}) for many ethylene isotopic species (see Refs.[34–43]). Because systematic "line-by-line" assignments remain quite tedious, the spectra of the minor ethylene isotopologues are much less studied than those of $^{12}C_2H_4$. As a direct consequence, most of the line positions and line intensities are clearly missing in available spectroscopic databases[44–46]. Fig. 1 shows a comparison between the observed (only 151 available) and our variationally predicted vibrational (1252 calculated energy levels) band centers for 11 isotopologues up to 3100 cm^{-1}. For the very first time, we provide first-principles "global" calculations for $^{12}CHD^{13}CH_2$, $^{13}CHD^{12}CH_2$, $^{12}C_2HD_3$ and $^{12}C_2D_4$. To our knowledge, there are no published experimental measurements for $^{12}CHD^{13}CH_2$ and $^{13}CHD^{12}CH_2$. A limited number of publications were devoted to the infrared spectra of $^{12}C_2HD_3$ and $^{12}C_2D_4$. The complete energy level redistribution under H $\rightarrow$ D substitution is clearly seen in the lower panel of Fig. 1. According to the type of substitution, the density of states will differ significantly (e.g. 213 vibrational states for $^{12}C_2D_4$ against only 73 states for $^{12}C_2H_4$ in the same spectral range 0$-$3100 cm^{-1}).

$^{12}C_2HD_3$: First measurements and assignments of the 12 fundamental vibrational modes of $^{12}CD_2^{12}CHD$ were carried out by Courtoy *et al.*[47,48] in the 50s and later on by Duncan *et al.*[49] at low resolution. In 1993, Duncan *et al.*[50] extended their work and assigned 33 vibrational transitions at a resolution of about 0.5 cm^{-1}. Martin *et al.*[51] have calculated the *ab initio* fundamental frequencies using augmented coupled cluster methods. The first high-resolution infrared spectra of ν_8 band was carried out by Tan *et al.*[52,53], initially at a resolution of 0.0063 cm^{-1}, which was improved reaching up to a resolution of 0.00096 cm^{-1} using the high-resolution synchrotron FTIR spectroscopy[34]. Three rotational constants, a quartic centrifugal constants and the value of the band center for the ν_6 band were also determined. Recently, Ng *et al.*[54] carried out the first analysis of $2\nu_8$ and its Coriolis interaction with the $\nu_3+\nu_4$.

$^{12}C_2D_4$: The first infrared spectra of some fundamental ($\nu_1, \nu_5, \nu_7, \nu_9, \nu_{11}, \nu_{12}$) and combination ($\nu_2+\nu_9, \nu_5+\nu_{11}, \nu_1+\nu_{11}$) bands of $^{12}C_2D_4$ were recorded and analyzed by Harper, Morrison, and Duncan[55–59] at a resolution of 0.02 cm^{-1}. A complete analysis of the Coriolis interacting tetrad of four fundamental bands (ν_4, ν_7, ν_{10}, ν_{12}) was obtained by Mose *et al.*[60] The Raman spectrum of ν_3 and ν_6 bands were further investigated in Ref.[61] The ro-vibrational analysis of the ν_9, ν_{11} and ν_{12} bands were carried out by Tan *et al.* at different resolutions (with uncertainty varying from 0.04 to 0.00096 cm^{-1}, see Refs.[62–65,65]).

Table 2 Small sample of variationally predicted vibrational band centers (in cm^{-1}) of *as*$-^{12}C_2H_2D_2$ based on the isotopic shifts from the "mother" molecule $^{12}C_2H_4$ denoted by VIS[1] and PMM $^{12}C_2H_3D$ denoted by VIS[2]. The Hamiltonian model $H(10-6)$ and $F(10)$ basis set were considered.

Band (Sym)	VIS[1]	VIS[2]	Pred[1]	Pred[2]	Obs-Pred[1]	Obs-Pred[2]
ν_{10} (B_{3u})	141.36	47.55	684.57	684.59	0.07	0.05
ν_8 (B_{3g})	-3.53	0.12	943.39	943.39	0.03	0.03
ν_7 (B_{2u})	198.28	55.85	750.49	750.63	0.08	-0.06
ν_6 (B_{2g})	85.14	-16.25	1140.27	1141.52	1.99	0.75
ν_{12} (B_{1u})	59.10	17.15	1383.34	1383.61	0.60	0.33
ν_2 (A_g)	40.57	19.51	1585.60	1585.99	0.45	0.06

Table 3 Small sample of theoretically predicted vibrational band centers (in cm^{-1}) of $^{12}CHD^{13}CH_2$ and $^{13}CHD^{12}CH_2$ based on the isotopic shifts from the "mother" $^{12}C_2H_4$ molecule denoted by VIS[1] and the PMM $^{12}C_2H_3D$ denoted by VIS[2] . The observed band centers are completely lacking in the literature.

	$^{12}CHD^{13}CH_2$				$^{13}CHD^{12}CH_2$			
Band (Sym)	VIS[1]	VIS[2]	Pred[1]	Pred[2]	VIS[1]	VIS[2]	Pred[1]	Pred[2]
ν_{10} (B_{3u})	93.972	0.171	731.954	731.974	95.720	1.918	730.207	730.226
ν_8 (B_{3g})	5.125	8.768	934.735	934.735	- 2.953	0.690	942.813	942.813
ν_7 (B_{2u})	142.669	0.236	806.102	806.237	150.246	7.813	798.525	798.659
ν_4 (A_u)	25.447	- 0.081	1000.142	1000.121	26.999	1.471	998.590	998.569
ν_3 (A_g)	61.769	6.871	1281.771	1281.918	58.370	3.471	1285.170	1285.317
ν_{12} (B_{1u})	42.025	0.075	1400.418	1400.688	52.208	10.258	1390.235	1390.505

3 Generalized method of vibrational isotopic shifts applied to all ethylene isotopologues

3.1 Vibrational isotopic shift procedure

In spectroscopy, most of the studies are generally devoted to main isotopologue (the most abundant species) that will be denoted as the "mother molecule" in the following. Contrary to the minor isotopic species, experimental and theoretical investigations (determination of the band centers, assignments, etc.) are much more important for the mother molecules for which results are regularly improved and updated in the well-known spectroscopic databases. However, the increasing number of experimental studies devoted to ethylene isotopologues makes necessary to have accurate theoretical predictions. In turn, these latter could be improved from experimentally-determined band centers using the VSS procedure[66]. So, in order to have access to a large amount of experimental informations, we have generalized in this work our previously reported vibrational isotopic shifts (VIS) method which was applied with success to methane[24,25], phosphine[67] and other ethylene isotopologues[27,28]. So far, the VIS method was based on the propagation of information from the mother (major species, called IsoA) molecule to a daughter (minor species, called IsoB) molecule. Typically, VIS was defined as the energy difference VIS=Calc(IsoA)-Calc(IsoB). Accurate knowledge of this VIS will help assigning and modelling more easily unknown ethylene bands. From the VIS and the experimental band centers of IsoA (if available), we can access to the "experimentally" lacking information for IsoB by applying the relation

$$\text{Pred(IsoB)= Obs(IsoA)- VIS} \tag{1}$$

where Pred(IsoB) can be considered as an "empirical observed value" for IsoB. This method is quite general and could be applied, in theory, to any isotopic substitution. However, for very pronounced isotopic changes due to one or more H $\rightarrow$ D substitutions, the determination of VIS may be less accurate. This can be simply explained by the fact that resonance interaction schemes for IsoA and IsoB may differ making convergence of variational calculations quite different. To overcome this problem, we propose to generalize the VIS method by considering, instead of IsoA, a molecular species IsoA' for which (*i*) the vibrational pattern is closer to that of IsoB and (*ii*) experimental data is available. We will denote IsoA' as a "pseudo mother" molecule (PMM) in the following. In this case, the isotopic vibrational shifts IsoA' $\leftrightarrow$ IsoB will be determined with better accuracy than for IsoA $\leftrightarrow$ IsoB (see Fig. 2). By this procedure, we have thus much more possibilities for propagating information to ensure accurate and consistent VIS. In turn, the same number of vibrational functions and a similar Hamiltonian model both for IsoA' and IsoB species have to be considered. In other words, variational calculations must be performed in the same point groups both for IsoA' and IsoB. In this context, the substitution of four H atoms by D or ^{12}C by ^{13}C does not alter the initial D_{2h} symmetry, while partial H $\rightarrow$ D and/or $^{12}C \rightarrow {}^{13}C$ substitutions will lead to three possible ethylene symmetry configurations, namely C_{2h}, C_{2v} and C_s. Here, all calculations have been carried out in the lowest C_s symmetry using the Hamiltonian model $H(10-6)$ (see Refs.[27,68] for the definition of the reduced model $H(m-n)$). To illustrate the method, Tab. 2 provides a small sample of variationally predicted vibrational band centers (in cm^{-1}) for $as-{}^{12}C_2H_2D_2$ ($\equiv$ IsoB) based on the isotopic shifts. Rather than using $^{12}C_2H_4$ ($\equiv$ IsoA), we preferred to consider $^{12}C_2H_3D$ ($\equiv$ IsoA') which is closer to $as-{}^{12}C_2H_2D_2$.

Table 2 corroborates the fact that starting from a PMM slightly improves accuracy of the predicted band centers for $as-C_2H_2D_2$ (see Obs-Pred[1] and Obs-Pred[2]). Tab. 3 provides a small sample of vibrational band centers for $^{12}CHD^{13}CH_2$

Table 4 Theoretically predicted vibrational band centers (in cm^{-1}) of $^{12}C^{13}CH_4$ based on the isotopic shifts considering as the "mother" molecule $^{12}C_2H_4$, $^{13}C_2H_4$ and $^{12}C_2H_3D$ denoted respectively as ^{1,2,3}. The Hamiltonian model $H(10-6)$ and $F(10)$ basis set were considered.

Band (Sym)	VIS^1	VIS^2	VIS^3	Pred^1	Pred^2	Pred^3	Obs-Pred^1	Obs-Pred^2	Obs-Pred^3
ν_{10} (B_{3u})	0.52	-0.49	-93.28	825.407	825.405	825.426	-0.001	0.001	-0.020
ν_8 (B_{3g})	7.66	-5.33	11.30	932.199		932.199	-0.004		-0.004
ν_7 (B_{2u})	1.33	-3.67	-141.10	947.442	947.437	947.576	0.003	0.008	-0.131
ν_4 (A_u)	-0.11	0.11	-25.63	1025.694	1025.698	1025.673	0.003	0.00004	0.024
ν_6 (B_{2g})	8.76	-8.84	-92.63	1216.654		1217.903	-1.654		-2.903
ν_3 (A_g)	6.66	-7.52	-48.24	1336.883		1337.030	-0.044		-0.192
ν_{12} (B_{1u})	3.09	-2.70	-38.86	1439.354	1439.355	1439.624	-0.008	-0.009	-0.278
ν_2 (A_g)	19.91	-20.67	-1.15	1606.265		1606.654	-0.171		-0.559
$2\nu_{10}$ (A_g)	2.49	-1.69	-193.48	1659.710			0.196		
ν_8+ν_{10} (A_u)	7.84	-6.13	-81.25	1758.825	1758.816				
ν_7+ν_{10} (B_{1g})	2.17	-3.84	-237.66	1778.837					
ν_4+ν_{10} (B_{3g})	0.46	-0.43	-119.00	1853.502					
$2\nu_8$ (A_g)	15.54	-10.23	22.31	1865.358					
ν_7+ν_8 (B_{1u})	8.31	-9.24	-130.94	1880.670	1880.665				
ν_4+ν_8 (B_{3u})	7.68	-5.04	-12.62	1950.607	1950.618				
ν_4+ν_7 (B_{2g})	1.05	-3.69	-159.74	1964.394					
ν_6+ν_7 (A_u)	9.78	-12.77	-236.31	2168.227					
ν_4+ν_6 (B_{2u})	8.66	-8.69	-118.44	2244.146					
ν_3+ν_7 (B_{2u})	8.10	-10.96	-187.35	2283.399					
$3\nu_{10}$ (B_{3u})	3.02	-2.40	-298.16	2501.262					
ν_2+ν_7 (B_{2u})	22.19	-24.56	-140.13	2549.585					
ν_7+$2\nu_{10}$ (B_{2u})	3.48	-4.511	-340.52	2619.373					
ν_2+ν_4 (A_u)	19.95	-20.43	-27.40	2624.880					
$2\nu_3$ (A_g)	13.75	-15.53	-98.92	2671.552					
ν_{11} (B_{1u})	7.89	-10.79	-707.25	2980.741	2980.393				
ν_1 (A_g)	5.74	-5.52	11.87	3016.114					
ν_5 (B_{2g})	8.44	-5.63	-12.66	3073.918					
ν_9 (B_{3u})	5.04	-5.90	-3.98	3099.830					

and $^{13}CHD^{12}CH_2$ based on the isotopic shifts using the observed band centers from $^{12}C_2H_4$ and $^{12}C_2H_3D$. We do not provide comparisons with observed band centers because they are completely lacking in the literature. In Tab. 4, the VIS method is applied to the $^{13}C^{12}CH_4$ isotopologue. To this end, we have considered three PMMs, namely $^{12}C_2H_4$, $^{13}C_2H_4$ and $^{12}C_2H_3D$, for which experimental data are available. VIS^1, VIS^2 and VIS^3 correspond respectively to the three VIS obtained with respect to $^{12}C^{13}CH_4$. We can clearly see that the precision of the corresponding Pred^1 and Pred^2 (see Eq. 1) is quite similar while Pred^3 leads to larger Obs-Pred^3 errors. It proves that this method is not suited for isotopic species whose geometrical structure considerably differs from the "mother" molecule. However, there are others factors to consider (assuming that all calculations are well-converged) in order to make this method efficient: the accuracy of experimentally determined band centers, the quality of the potential energy surface used in variational calculations, the vibrational states in strong resonance, etc. This last factor may have a significant impact on the precision of the isotopic shift method. As an illustration, let us consider the band ν_{11} of $^{13}C^{12}CH_4$ (see Tab. 4) whose the first two terms in the eigenfunction decomposition are $0.794|v_{11}=1\rangle + 0.486|v_2=1, v_{12}=1\rangle + \cdots$. The resonance of the vibrational state $|v_{11}=1\rangle$ with $|v_2=1, v_{12}=1\rangle$ makes the error between Pred^1 and Pred^2 more pronounced, that is 0.35 cm^{-1} against 0.001-0.01 cm^{-1} for other vibrational "isolated" bands. Unless a specific treatment (e.g. use of effective Hamiltonian), such accidental resonances are generally quite difficult to control for such 6-atomic systems and may have an impact both on the convergence of the energy levels and on intensity borrowing. However, though less accurate, the isotopic shifts remain quite relevant to refine band centers. In Tab. 5, we aim to provide the most accurate values for a sample of 25 band centers corresponding to 11 ethylene isotopologues resulting either from VIS (with symbols †, ^{M} or *), direct variational calculations (denoted as ^{V}) or from analyses (no symbol). The predicted band centers deduced from PMM are denoted by †, those obtained from the mother molecule $^{12}C_2H_4$ are denoted by ^{M} while "*" means that the band centers have been obtained as an average of different band centers deduced from very similar PMM. For example, the $\nu_7+\nu_8$ band center was determined for

Table 5 Vibrational band centers (in cm^{-1}) for 11 ethylene isotopologues. The predicted band centers deduced from PMM are denoted by †, those obtained from the mother molecule $^{12}C_2H_4$ by ^{M} and by * the band centers obtained by as an average of different band centers deduced from very similar PMM.

Band (Sym)	$^{12}C_2H_4$	$^{12}C^{13}CH_4$	$^{13}C_2H_4$	$^{12}C^{13}CH_3D$	$^{13}C^{12}CH_3D$	$^{12}C_2H_3D$	cis	trans	as	$^{12}C_2HD_3$	$^{12}C_2D_4$
ν_1 (A_g)	3021.855	3016.114†	3010.597^{M}	3016.657^{M}	3018.524^{M}	3027.986^{M}	2300.535	2284.854*	3017.12	2281.956*	2261.950^{V}
ν_2 (A_g)	1626.17	1606.095	1585.422†	1580.930†	1588.223†	1605.5	1571.202†	1571.075†	1586.051	1548.109†	1517.644^{V}
ν_3 (A_g)	1343.54	1336.838	1329.320†	1281.918†	1285.317†	1288.789	1218.136†	1285.171†	1030.07	1043.217*	984.864
ν_4 (A_u)	1025.589	1025.698	1025.804	1000.121†	998.569†	1000.039	980.364	987.753	890.397*	763.655*	729.958
ν_5 (B_{2g})	3082.36	3073.918†	3068.292^{M}	3057.304^{M}	3050.764^{M}	3061.254^{M}	3054.735	3046.639†	2334.587†	2221.738†	2314.570^{V}
ν_6 (B_{2g})	1225.41	1216.654†	1207.816^{M}	1116.737†	1120.613†	1125.277	1039.768	1003.891†	1142.27	998.917	1003.347†
ν_7 (B_{2u})	948.77	947.445	943.763	806.237†	798.659†	806.473	842.210	724.755	750.568	724.087*	719.771
ν_8 (B_{3g})	939.86	932.196	926.865†	934.735†	942.813†	943.5033	759.958	863.127*	943.413	918.733	778.458†
ν_9 (B_{3u})	3104.872	3099.830†	3093.927^{M}	3084.302^{M}	3095.249^{M}	3095.854^{M}	3060.423	3065.2	3094.114	3048.673*	2341.837
ν_{10} (B_{3u})	825.93	825.406	824.915	731.974†	730.226†	732.144	662.872	673.535	684.642	628.991*	593.344
ν_{11} (B_{1u})	2988.631	2980.569*	2969.602	2269.733^{M}	2259.989^{M}	2273.492^{M}	2252.80	2276.263*	2230.545	2331.578*	2200.980
ν_{12} (B_{1u})	1442.44	1439.346	1436.654	1400.688†	1390.505†	1400.763	1341.151	1298.038	1383.944	1288.552*	1076.985
$\nu_8+\nu_{10}$ (A_u)	1766.665	1758.821*	1752.684	1668.678^{M}	1674.947^{M}	1677.571^{M}	1423.599†	1536.938	1629.900†	1548.786†	1372.407^{V}
$\nu_7+\nu_8$ (B_{1u})	1888.978	1880.668*	1871.428	1740.687^{M}	1741.262^{M}	1749.729^{M}	1599.420	1586.162	1696.784*	1644.415*	1496.289^{V}
$\nu_6+\nu_{10}$(B_{1u})	2047.776	2038.524†	2029.223^{M}	1846.120^{M}	1848.491^{M}	1855.040^{M}	1697.576†	1674.595	1823.516†	1626.213†	1593.157^{V}
$\nu_6+\nu_7$ (A_u)	2178.011	2168.227†	2155.461^{M}	1923.214^{M}	1919.548^{M}	1931.915^{M}	1880.507†	1727.177	1892.537†	1722.063†	1723.205^{V}
$\nu_4+\nu_8$ (B_{3u})	1958.282	1950.613*	1945.575	1929.367^{M}	1935.761^{M}	1937.989^{M}	1740.306†	1845.987	1826.665†	1681.918†	1505.009^{V}
$\nu_3+\nu_7$ (B_{2u})	2291.5	2283.399†	2272.436^{M}	2088.829^{M}	2084.681^{M}	2096.053^{M}	2062.113^{M}	2010.745^{M}	1780.756^{M}	1768.333^{V}	1704.188^{V}
$2\nu_{10}$ (A_g)	1662.2	1659.906	1658.221†	1465.573^{M}	1462.12^{M}	1466.229^{M}	1330.636	1352.039*	1371.493	1260.810*	1191.218^{V}
$\nu_4+\nu_7$ (B_{2g})	1965.44	1964.394†	1960.701^{M}	1804.449^{M}	1795.286^{M}	1804.654^{M}	1816.358	1713.456†	1635.073†	1484.895†	1445.637^{V}
$\nu_6+\nu_8$ (B_{1g})	2169.946^{V}	2153.516^{V}	2139.663^{V}	2053.900^{V}	2065.905^{V}	2071.181^{V}	1798.060	1864.250†	2085.815†	1914.788†	1783.141^{V}
$\nu_2+\nu_7$ (B_{2u})	2571.77	2549.585†	2525.024^{M}	2384.839^{M}	2384.620^{M}	2409.457^{M}	2410.532^{M}	2294.140^{M}	2335.448^{M}	2269.676†	2235.425
$2\nu_4$ (A_g)	2047.759	2047.959†	2048.162^{M}	1994.178^{M}	1991.296^{M}	1994.162^{M}	1954.760^{M}	1964.924^{M}	1778.248^{M}	1524.161^{V}	1458.230^{V}
$\nu_4+\nu_{10}$(B_{3g})	1853.96	1853.502†	1853.075^{M}	1734.392^{M}	1731.086^{M}	1734.500^{M}	1644.11^{M}	1663.781^{M}	1576.889^{M}	1393.674^{V}	1324.372^{V}
$2\nu_7$ (A_g)	1899.75	1896.991†	1889.805^{M}	1610.146^{M}	1595.459^{M}	1610.587^{M}	1685.499†	1446.364†	1499.410	1444.812†	1440.126^{V}

$^{12}C^{13}CH_4$ by an average of 1880.67015 cm^{-1} obtained from the mother molecule $^{12}C_2H_4$ and 1880.66512 cm^{-1} when $^{13}C_2H_4$ was considered.

3.2 Correspondence between vibrational levels

The key point of the VIS approach is to properly link vibrational levels between different species. In other words, we have to be able to predict the evolution of the state A (or A') toward another state B. In general, such connection is not direct, in particular in presence of strong resonances or/and due to important changes of mass. Instead of considering drastic changes between IsoA (or IsoA') and IsoB, a way to proceed is to vary the masses almost continuously. In other words, variational calculations have to be performed on the grid $m_A, m_A+\delta, m_A+2\delta, \cdots, m_B$ with $\delta << m_A$ and m_B. As a simple illustration, Fig. 3 shows the evolution of the harmonic frequencies for five ethylene isotopologues from quasi-continuous H $\rightarrow$ D substitutions from $^{12}C_2H_4$ to $^{12}C_2D_4$. Each point on this figure corresponds to an intermediate mass m' between m_A and m_B. Note that we have used the following atomic masses $m_H = 1.0078250321$ a.u., $m_D = 2.0141017780$ a.u., $m_{^{12}C} = 12$ a.u. and 18 intermediate masses have been considered. As depicted in this figure, all the correspondences are now clearly established, even for brutal changes (see e.g. w_1 and w_{11}). In Tab. 6 we provide harmonic frequencies for 5 ethylene isotopologues corresponding to the full line of Fig. 3.

4 Computational models for energy level and intensity calculations

Following our previous works[24,28,69] a reduced form of the Watson-Eckart Hamiltonian in normal coordinates was employed[70]. This Hamiltonian was initially Taylor-expanded up to order $n = 10$ and then reduced at order $m = 6$ resulting in the $H(10-6)$ Hamiltonian model for all ethylene isotopologues. The total number of Hamiltonian operators was only 10882 for the D_{2h} species $^{12}C_2D_4$ against $\approx$ 107 000 operators for the C_s isotopologues. Vibrational calculations were performed using the cut-off criterion as follows: $F_{k_i}(v_{\max}) \Leftrightarrow \sum k_i v_i \leq v_{\max}$ where k_i ($i = 1, \cdots, 12$) stand for weight coefficients and $v_i = 0, \cdots, v_{\max}$. The weight coefficients were chosen to select 7, 8 and 10 basis functions for the stretching, bending and torsional modes for all 3 C_s isotopologues ($^{12}CHD^{13}CH_2$, $^{13}CHD^{12}CH_2$ and $^{12}C_2HD_3$). For the D_{2h} isotopologue ($^{12}C_2D_4$), the k_i coefficients were chosen to select 9 functions for stretching and 11 for bending and torsional modes. To ensure that the memory necessary to store the A' and A'' blocks for diagonalization does not exceed 100 Gb, the rovibrational calculations were splitted for C_s isotopologues in two parts : for $1 < J < 18$, calculations were carried out using the $F(10-6)$ basis and for $19 < J < 30$ the $F(10-5)$ basis was

Table 6 Calculated harmonic frequencies of $^{12}C_2H_4$, $^{12}C_2H_3D$, *cis*$-^{12}C_2H_2D_2$, $^{12}C_2HD_3$ and $^{12}C_2D_4$. S. and A. stand for "symmetric" and "antisymmetric". All values are given in cm^{-1}.

	($Sym = D_{2h}$) Description†	$^{12}C_2H_4$	$^{12}C_2H_3D$	*cis*$-^{12}C_2H_2D_2$	$^{12}C_2HD_3$	$^{12}C_2D_4$
ω_1	(A_g) S. CH stretch	3159.355	3151.307	2374.690	2363.201	2335.502
ω_2	(A_g) CC stretch	1673.811	1644.751	1606.808	1579.701	1548.922
ω_3	(A_g) S. HCH bend	1370.120	1313.760	1241.048	1061.270	1002.208
ω_4	(A_u) H_2C–CH_2 torsion	1051.450	1023.745	1000.678	936.929	743.773
ω_5	(B_{2g}) trans CH stretch	3225.390	3196.283	3187.506	2413.807	2405.222
ω_6	(B_{2g}) A. HCH wag	1247.904	1142.722	1054.883	1013.049	1015.796
ω_7	(B_{2u}) S. out of plane bend	965.646	959.993	856.174	735.592	730.475
ω_8	(B_{3g}) A. out of plane bend	955.743	819.426	772.233	775.525	789.438
ω_9	(B_{3u}) cis CH stretch	3251.893	3240.999	3208.553	3198.196	2421.509
ω_{10}	(B_{3u}) S. HCH wag	828.462	734.663	665.524	631.043	595.336
ω_{11}	(B_{1u}) A. CH stretch	3144.151	2355.270	2335.535	2294.605	2270.347
ω_{12}	(B_{1u}) A. HCH bend	1479.819	1433.755	1370.139	1313.772	1096.628

† Types of vibrations for $^{12}C_2H_4$. According to the bond length involved in the vibration, they will change for each isotopologue.

considered. To ensure good convergence of ro-vibrational levels and partition function for $^{12}C_2D_4$, ro-vibrational calculations were carried out up to $J = 35$ using the $F(11-6)$ basis set. The total internal partition function at a given temperature is given by

$$Q(T) = \sum_{v,J} (2J+1) g_C e^{-c_2 E_{vJ}/T}, \tag{2}$$

where E_{vJ} are our variationally-computed energy levels, c_2 corresponds to the factor $hc/k = 1.4388$ cm·K with k the Boltzman constant and g_C are the nuclear spin statistical weights. For $^{12}C_2D_4$, we have obtained $g_A = 27$ ($A \equiv A_g, A_u$) and $g_B = 18$ ($B \equiv B_{1g}, B_{2g}, B_{3g}, B_{1u}, B_{2u}, B_{3u}$). Concerning $^{12}C_2HD_3$ and $^{12}CHD^{13}CH_2$/ $^{13}CHD^{12}CH_2$ we have determined, respectively, $g_{A'} = g_{A''} = 54$ and $g_{A'} = g_{A''} = 48$. For C_s isotopologues, we have obtained Q(296 K) =163 855.9 for $^{12}C^{13}CH_3D$, Q(296 K)= 163 252.5 for $^{13}C^{12}CH_3D$ and Q(296 K) = 262 884.9 for $^{12}C_2HD_3$ up to $J = 30$. After a simple convergence test (error between $Q_{J=30}$ and $Q_{J=29}$), we have estimated that the error on Q does not exceed 1.0% at 296 K. For $^{12}C_2D_4$, we have obtained Q(296 K) = 120 985.2 with an error estimated at $\approx 0.5\%$. The two quantities (Q, g_C) are necessary for the computation of the infrared line intensities given in $cm^{-1}/(cm^{-2}$ molecule$^{-1}) \equiv$ cm/molecule

$$S_{if} = \frac{8\pi^3 10^{-36}}{3hcQ(T)} g_C \nu_{if} e^{-c_2 E_i/T} (1 - e^{-c_2 \nu_{if}/T}) \mathscr{R}_{if}, \tag{3}$$

where E_i is the lower state energy. The ν_{if} is the rovibrational transition wavenumber (in cm^{-1}), $\mathscr{R}_{if}$ is the line strength (square of the absolute value of the ro-vibrational matrix elements of the dipole moment). The probability of a transition $i \leftarrow f$ is given by the square of the transition-moment matrix elements by summing over all magnetic sublevels of both initial and final states

$$\mathscr{R}^{\theta}_{if} \equiv \sum_{M_i, M_f} | \langle \Psi^{(J_i, C_i)}_{v_i, M_i} | \mu^{\mathbf{L}}_{\theta} | \Psi^{(J_f, C_f)}_{v_f, M_f} \rangle |^2, \tag{4}$$

where $\theta = X, Y, Z$ are the space-fixed electronic dipole moment components. Due to the isotropy of space, only the Z component is necessary such that $\mathscr{R}_{if} = \mathscr{R}^X_{if} + \mathscr{R}^Y_{if} + \mathscr{R}^Z_{if} \equiv 3\mathscr{R}^Z_{if}$. In that case, we write

$$\mu^L_Z = \sum_{\alpha} \lambda_{Z\alpha} \mu^M_{\alpha}, \tag{5}$$

where $\lambda_{Z\alpha}$ are the direction cosines[71–73] and μ^M_{α} are the *ab initio* molecule-fixed dipole moment components ($\alpha = x, y, z$). For matrix element calculations, it is computationally advantageous to consider the spherical tensor formalism and Wigner D-functions (see e.g.[72]). Here, we have considered the 12D ethylene DMS reported by Delahaye *et al.* in Ref.[31] which was originally expressed in symmetry-adapted D_{2h} normal coordinates. The normal mode VQZ 4th order ethylene DMS $\mu_{\alpha}(q)$ ($\alpha = x, y, z$) has been rewritten in terms of the q'_i(Iso) coordinates and expanded to third order without any refitting procedures using the nonlinear transformation given in Refs.[25,26,67]. The symmetry branching rules are deduced in a straightforward manner from $(\mu_x^{(B_{3u})}, \mu_y^{(B_{2u})}, \mu_z^{(B_{1u})})_{D_{2h}}$ using the correlation table: $(B_{3u}) \rightarrow A'$, $(B_{2u}) \rightarrow A''$ and $(B_{1u}) \rightarrow A'$.

5 *Ab initio* rovibrational intensity predictions and comparison with observed spectra

For the first time, accurate theoretical line positions and line intensities are computed for $^{12}CHD^{13}CH_2$, $^{13}CHD^{12}CH_2$, $^{12}C_2HD_3$ and $^{12}C_2D_4$ ethylene isotopologues in the range $[0-4500\ cm^{-1}]$. The corresponding line lists are summarized in Fig. 4 where the main $^{12}C_2H_4$ isotopologue has been added (top panel). We clearly see in this figure the impact of the successive isotopic substitutions on the global shape of the spectra with a reorganization of the vibrational bands and polyad structure. In Tabs. 7, 8,9, 10, we provide a sample of theoretical line intensities and Einstein coefficients *A* for the strongest transitions. The best way to validate quality and accuracy of our variational predictions is to make direct comparisons with experiment, when available, except for $^{12}CHD^{13}CH_2$ and $^{13}CHD^{12}CH_2$ whose spectra have not been yet measured. As expected and as confirmed in Fig. 4, the shape of the spectrum of these two species is quite similar to that of $^{12}C_2H_3D$[27]. Fig. 5 gives comparisons of transmittance spectra between $^{12}C_2H_3D$, $^{12}CHD^{13}CH_2$ and $^{13}CHD^{12}CH_2$. We note that the vibrational isotopic displacement with respect to $^{12}C_2H_3D$ is more pronounced for $^{13}CHD^{12}CH_2$. For $3-d$ ethylene, we show in Fig. 6 a very good agreement between the simulated spectrum ad the experiment[53] in the region of the ν_8 band. Recently, the $2\nu_8$ of $^{12}C_2HD_3$ band was analysed by Ng *et al.*[54]. Figs. 7 and 8 display two comparisons between variational-predicted and experimental spectra[54] and show the good qualitative agreement. The ν_{12} and ν_9 bands of $^{12}C_2D_4$ were analysed by Tan *et al.* in Refs.[62,64,74] The survey spectrum of ν_{12} band obtained by our variational calculations is given in Fig. 9 (left) and compared to the experimental spectrum on the right-hand side. The detailed portion of the *P* branch is plotted in Fig. 10 where the corresponding experimental spectrum is taken from Ref.[74] The large spectral range involving the *Q* branch of the ν_{12} band and located around 1078 cm^{-1} is shown in Fig. 11 (see also Fig. 12 for a detailed portion). The *R* branch region portion is displayed in Fig. 13 and compared to the experimental spectrum taken from Ref.[64] Once again, we note a good agreement between theory and experiment. Finally, the detailed portions of the ν_9 band are given in Figs. 14 and 15 where comparisons with experiment show a qualitative good agreement.

6 Conclusion

This paper gives a general insight of rotationally resolved spectra for eleven ethylene isotopic species obtained from accurate global variational calculations. In this work, we have completed our previous studies with four additional species – $^{12}C_2HD_3$, $^{12}C_2D_4$, $^{12}CHD^{13}CH_2$ and $^{13}CHD^{12}CH_2$ – for which the first two molecules contributed to the derivation of the full chain of successive $H \rightarrow D$ substitutions (in total, 6 different deuterated ethylene species were considered). To make calculations tractable for such 6-atomic systems, we have applied all our previous techniques (reduction/compression, nonlinear transformations between normal coordinates) and built our normal mode reduced models and basis-sets. The study of the most abundant ^{13}C enriched ethylene species was the topic of our previous paper[27]. Here, we give the first theoretical predictions for the ^{13}C and D enriched isotopologues $^{12}CHD^{13}CH_2$, $^{13}CHD^{12}CH_2$ for which no experimental data is available. All calculated line positions and intensities will be included in the freely accessible TheoReTS database[29]. In order to predict accurately unpublished vibrational band centers, we have proposed a general method based on the propagation of information between a "pseudo" mother and a "daughter" molecule. This generalizes the vibrational isotopic shift method reported elsewhere[24,25,28,67]. To properly make correspondence between vibrational states of different species, we have also introduced intermediate masses in the variational calculations.

Conflicts of interest

There are no conflicts to declare.

Acknowledgments

The support from French ANR e-PYTHEAS project (Grant 16-CE31-0005-04), from French-Russian joint Laboratory LIA "SAMIA", from Academic D.A. Mendeleev program of Tomsk State University, from Russian RFBR grant (19-03-00581) and from computing centers (ROMEO Champagne-Ardenne; IDRIS CNRS France) are acknowledged.

References

1 J. Aguilera and L. Whigham, *Isotopes in Environmental and Health Studies*, 2018, **54**, 573–587.

Table 7 Selected strong transitions for $^{12}C_2D_4$ computed at $T = 296$ K. A is the Einstein coefficient (in 1/s) and $E_{\rm low}$ is the lower state energy."l" and "u" stand for lower and upper states.

$\tilde{\nu}$(cm^{-1})	I(cm/mol)	A(1/s)	$E_{\rm low}$(cm^{-1})	$(JK_aK_c,C)^l$	$(JK_aK_c,C)^u$	Band
718.445	1.252×10^{-20}	1.535	91.620	11 2 10, A_g	11 1 10, A_u	ν_7
719.120	1.473×10^{-20}	1.795	122.938	13 2 12, A_g	13 1 12, A_u	ν_7
719.359	1.082×10^{-20}	2.329	35.457	7 1 7, B_{3g}	7 0 7, B_{3u}	ν_7
719.731	1.450×10^{-20}	2.606	67.447	10 1 10, B_{2g}	10 0 10, B_{2u}	ν_7
719.802	1.525×10^{-20}	2.665	80.392	11 1 11, B_{3g}	11 0 11, B_{3u}	ν_7
719.959	2.366×10^{-20}	2.717	94.425	12 0 12, A_g	12 1 12, A_u	ν_7
719.964	1.528×10^{-20}	2.671	80.317	11 0 11, B_{1g}	11 1 11, B_{1u}	ν_7
719.987	2.181×10^{-20}	2.614	67.327	10 0 10, A_g	10 1 10, A_u	ν_7
720.037	1.357×10^{-20}	2.545	55.451	9 0 9, B_{1g}	9 1 9, B_{1u}	ν_7
720.122	1.853×10^{-20}	2.458	44.685	8 0 8, A_g	8 1 8, A_u	ν_7
720.159	1.394×10^{-20}	2.899	224.617	19 1 19, B_{3g}	19 0 19, B_{3u}	ν_7
720.162	1.394×10^{-20}	2.899	224.616	19 0 19, B_{1g}	19 1 19, B_{1u}	ν_7
720.206	1.316×10^{-20}	2.914	247.714	20 1 20, B_{2g}	20 0 20, B_{2u}	ν_7
1061.886	1.074×10^{-21}	0.451	105.788	12 1 1, B_{3g}	11 1 10, B_{3u}	ν_{12}
1062.204	1.038×10^{-21}	0.438	106.692	12 2 11, B_{1g}	11 2 10, B_{1u}	ν_{12}
1064.044	1.044×10^{-21}	0.426	80.317	11 0 11, B_{1g}	10 0 10, B_{1u}	ν_{12}
1067.380	1.354×10^{-21}	0.436	44.685	8 0 8, A_g	7 0 7, A_u	ν_{12}
1077.807	1.456×10^{-21}	0.693	91.750	6 6 0, A_g	6 6 1, A_u	ν_{12}
1078.435	1.407×10^{-21}	0.719	161.329	8 8 0, A_g	8 8 1, A_u	ν_{12}
1079.233	1.152×10^{-21}	0.736	250.360	10 10 0, A_g	10 0 1, A_u	ν_{12}
1085.579	1.179×10^{-21}	0.359	26.486	6 0 6, A_g	7 0 7, A_u	ν_{12}
1091.102	1.043×10^{-21}	0.375	80.392	11 1 11, B_{3g}	12 1 12, B_{3u}	ν_{12}
1091.133	1.041×10^{-21}	0.375	80.317	11 0 11, B_{1g}	12 0 12, B_{1u}	ν_{12}
1092.247	1.582×10^{-21}	0.377	94.424	12 0 12, A_g	13 0 13, A_u	ν_{12}
2180.839	1.171×10^{-21}	2.180	178.605	16 2 15, B_{1g}	15 2 14, B_{1u}	ν_{11}
2182.410	1.155×10^{-21}	2.183	153.140	14 3 12, B_{2g}	13 3 11, B_{2u}	ν_{11}
2183.045	1.264×10^{-21}	2.243	139.915	14 1 13, B_{3g}	13 1 12, B_{3u}	ν_{11}
2183.173	1.360×10^{-21}	2.286	143.476	15 0 15, B_{1g}	14 0 14, B_{1u}	ν_{11}
2184.350	1.386×10^{-21}	2.300	126.020	14 1 14, B_{2g}	13 1 13, B_{2u}	ν_{11}
2185.809	1.136×10^{-21}	2.178	103.725	11 3 8, B_{2g}	10 3 7, B_{2u}	ν_{11}
2187.291	1.096×10^{-21}	2.164	88.830	10 3 7, B_{3g}	9 3 6, B_{3u}	ν_{11}
2188.452	1.145×10^{-21}	2.287	68.002	9 2 7, B_{1g}	8 2 6, B_{1u}	ν_{11}
2190.203	1.168×10^{-21}	1.830	75.635	8 4 4, A_g	7 4 3, A_u	ν_{11}
2190.602	1.079×10^{-21}	2.281	53.577	8 2 7, B_{1g}	7 2 6, B_{1u}	ν_{11}
2191.234	1.787×10^{-21}	2.413	44.685	8 0 8, A_g	7 0 7, A_u	ν_{11}
2192.545	1.085×10^{-21}	2.427	35.457	7 1 7, B_{3g}	6 1 6, B_{3u}	ν_{11}
2199.971	1.120×10^{-21}	3.369	73.053	9 8 1, B_{1g}	9 8 2, B_{1u}	ν_{11}
2200.002	1.330×10^{-21}	4.222	61.329	8 8 1, B_{1g}	8 8 0, B_{1u}	ν_{11}

2 A. Kohen and H.-H. Limbach, *Isotope effects in chemistry and biology*, 2005, pp. 1–1075.

3 M. Wolfsberg, W. Alexander Van Hook, P. Paneth and L. Rebelo, *Isotope effects: In the chemical, geological, and bio sciences*, 2009, pp. 1–466.

4 T. Kostiuk, *Infrared Physics and Technology*, 1994, **35**, 243–266.

5 P. Romani, D. Jennings, G. Bjoraker, P. Sada, G. McCabe and R. Boyle, *Icarus*, 2008, **198**, 420–434.

6 D. Jennings, R. Achterberg, B. Bézard, G. Bjoraker, J. Brasunas, R. Carlson, A. Coustenis, F. Flasar, P. Irwin, V. Kunde, A. Mamoutkine, C. Nixon, G. Orton, J. Pearl, P. Romani, M. Segura, A. Simon-Miller, E. Wishnow and S. Vinatier, *Optics InfoBase Conference Papers*, 2007.

7 J. Moses, B. Bézard, E. Lellouch, G. Gladstone, H. Feuchtgruber and M. Allen, *Icarus*, 2000, **143**, 244–298.

8 B. Hesman, G. Bjoraker, P. Sada, R. Achterberg, D. Jennings, P. Romani, A. Lunsford, L. Fletcher, R. Boyle, A. Simon-Miller,

Table 8 Selected strong transitions for $^{12}C_2HD_3$ computed at $T = 296$ K. A is the Einstein coefficient (in 1/s) and E_{low} is the lower state energy. "l" and "u" stand for lower and upper states.

$\tilde{\nu}$(cm^{-1})	I(cm/mol)	A(1/s)	E_{low}(cm^{-1})	$(JK_aK_c,C)^l$	$(JK_aK_c,C)^u$	Band
723.865	1.036×10^{-20}	1.532	49.038	8 1 8, A'	8 0 8, A''	ν_7
724.045	1.136×10^{-20}	1.591	60.644	9 1 9, A''	9 0 9, A'	ν_7
724.189	1.214×10^{-20}	1.638	73.499	10 1 10, A'	10 0 10, A''	ν_7
724.304	1.269×10^{-20}	1.675	87.596	11 1 11, A''	11 0 11, A'	ν_7
724.399	1.303×10^{-20}	1.705	102.932	12 1 12, A'	12 0 12, A''	ν_7
724.480	1.316×10^{-20}	1.729	119.503	13 1 13, A''	13 0 13, A'	ν_7
724.552	1.310×10^{-20}	1.747	137.305	14 1 14, A'	14 0 14, A''	ν_7
724.586	1.304×10^{-20}	1.706	102.839	12 0 12, A'	12 1 12, A''	ν_7
724.591	1.270×10^{-20}	1.676	87.454	11 0 11, A''	11 1 11, A'	ν_7
724.601	1.316×10^{-20}	1.729	119.443	13 0 13, A''	13 1 13, A'	ν_7
724.619	1.288×10^{-20}	1.763	156.338	15 1 15, A''	15 0 15, A'	ν_7
847.668	1.032×10^{-21}	0.914	417.218	12 12 0, A'	11 11 0,A''	ν_8
847.668	1.032×10^{-21}	0.914	417.218	12 12 1, A''	11 11 1,A'	ν_8
849.883	1.016×10^{-21}	0.729	406.027	14 11 4, A'	13 10 4,A''	ν_8
849.883	1.016×10^{-21}	0.729	406.027	14 11 3, A''	13 10 3,A'	ν_8
851.308	1.108×10^{-21}	0.783	386.385	13 11 3, A''	12 10 3,A'	ν_8
852.731	1.203×10^{-21}	0.849	368.151	12 11 2, A'	11 10 2,A''	ν_8
854.153	1.301×10^{-21}	0.929	351.322	11 11 0, A'	10 10 0,A''	ν_8
854.891	1.167×10^{-21}	0.681	361.224	14 10 4, A'	13 9 4,A''	ν_8
856.316	1.267×10^{-21}	0.729	341.572	13 10 3, A''	12 9 3,A'	ν_8
857.739	1.370×10^{-21}	0.786	323.328	12 10 3, A''	11 9 3,A'	ν_8
858.416	1.206×10^{-21}	0.601	341.757	15 9 6, A'	14 8 6,A''	ν_8
859.840	1.311×10^{-21}	0.636	320.679	14 9 5, A''	13 8 5,A'	ν_8
2383.284	4.117×10^{-22}	1.056	214.152	10 8 2, A'	11 9 3,A''	ν_{11}
2383.549	5.702×10^{-22}	1.270	232.717	13 7 6, A'	14 8 7,A''	ν_{11}
2394.627	4.294×10^{-22}	1.441	341.757	15 9 6, A'	16 10 7,A''	ν_{11}
2394.802	5.263×10^{-22}	1.974	323.328	12 10 3, A''	13 11 2,A'	ν_{11}
2396.212	4.739×10^{-22}	1.811	341.572	13 10 4, A'	14 11 3,A''	ν_{11}
2397.510	5.445×10^{-22}	2.533	351.322	11 11 1, A''	12 12 0,A'	ν_{11}
2397.616	3.441×10^{-22}	1.294	388.168	17 9 8, A'	18 10 9,A''	ν_{11}
2400.698	3.391×10^{-22}	1.465	404.758	16 10 6, A'	17 11 7,A''	ν_{11}
2401.399	3.679×10^{-22}	1.807	406.027	14 11 4, A'	15 12 3,A''	ν_{11}
2403.012	4.369×10^{-22}	2.605	417.218	12 12 0, A'	13 13 1,A''	ν_{11}
2404.283	3.858×10^{-22}	2.342	435.445	13 12 2, A'	14 13 1,A''	ν_{11}
2409.810	3.142×10^{-22}	2.556	508.364	14 13 2, A'	15 14 1,A''	ν_{11}

C. Nixon and P. Irwin, *Astrophys. J.*, 2012, **760**, 24.

9 R. Hu and S. Seager, *Astrophys. J.*, 2014, **784**, 63.

10 A. Coustenis, R. Achterberg, B. Conrath, D. Jennings, A. Marten, D. Gautier, C. Nixon, F. Flasar, N. Teanby, B. Bézard, R. Samuelson, R. Carlson, E. Lellouch, G. Bjoraker, P. Romani, F. Taylor, P. Irwin, T. Fouchet, A. Hubert, G. Orton, V. Kunde, S. Vinatier, J. Mondellini, M. Abbas and R. Courtin, *Icarus*, 2007, **189**, 35–62.

11 A. Coustenis and B. Bézard, *Icarus*, 1995, **115**, 126–140.

12 A. Coustenis, B. Bézard, D. Gautier, A. Marten and R. Samuelson, *Icarus*, 1991, **89**, 152–167.

13 S. Vinatier, B. Bézard, C. Nixon, A. Mamoutkine, R. Carlson, D. Jennings, E. Guandique, N. Teanby, G. Bjoraker, F. Michael Flasar and V. Kunde, *Icarus*, 2010, **205**, 559–570.

14 J. Kaye, *Rev. Geophys.*, 1987, **25**, 1609–1658.

15 J. Linsky, B. Draine, H. Moos, E. Jenkins, B. Wood, C. Oliveira, W. Blair, S. Friedman, C. Gry, D. Knauth, J. Kruk, S. Lacour, N. Lehner, S. Redfield, J. Shull, G. Sonneborn and G. Williger, *Astrophys. J.*, 2006, **647**, 1106–1124.

16 E. Lellouch, *European Space Agency, (Special Publication) ESA SP*, 2001, 287–294.

Table 9 Selected strong transitions for $^{12}CHD^{13}CH_2$ computed at $T = 296$ K. A is the Einstein coefficient (in 1/s) and E_{low} is the lower state energy."l" and "u" stand for lower and upper states.

$\tilde{\nu}$(cm^{-1})	I(cm/mol)	A(1/s)	E_{low}(cm^{-1})	$(JK_aK_c,C)^l$	$(JK_aK_c,C)^u$	Band
805.307	1.055×10^{-21}	1.402	58.300	8 1 8, A'	8 0 8, A''	ν_7
805.919	1.222×10^{-21}	1.515	87.173	10 1 10, A'	10 0 10, A''	ν_7
806.167	1.269×10^{-21}	1.559	103.836	11 1 11, A''	11 0 11, A'	ν_7
806.875	1.224×10^{-21}	1.659	185.208	15 1 15, A''	15 0 15, A'	ν_7
807.013	1.166×10^{-21}	1.669	209.212	16 1 16, A'	16 0 16, A''	ν_7
807.210	1.168×10^{-21}	1.672	209.111	16 0 16, A'	16 1 16, A''	ν_7
807.240	1.273×10^{-21}	1.564	103.308	11 0 11, A''	11 1 11, A'	ν_7
807.275	1.097×10^{-21}	1.676	234.604	17 0 17, A''	17 1 17, A'	ν_7
807.355	1.227×10^{-21}	1.521	86.466	10 0 10, A'	10 1 10, A''	ν_7
932.609	1.001×10^{-21}	2.337	26.227	5 1 5, A''	5 0 5, A'	ν_8
932.922	1.194×10^{-21}	2.469	35.410	6 1 6, A'	6 0 6, A''	ν_8
934.397	1.940×10^{-21}	3.245	141.587	13 1 13, A''	13 0 13, A'	ν_8
934.626	1.696×10^{-21}	3.444	234.674	17 1 17, A''	17 0 17, A'	ν_8
935.069	1.938×10^{-21}	3.183	121.587	12 0 12, A'	12 1 12, A''	ν_8
935.391	1.821×10^{-21}	3.003	86.466	10 0 10, A'	10 1 10, A''	ν_8
936.185	1.396×10^{-21}	2.633	44.616	7 0 7, A''	7 1 7, A'	ν_8
936.511	1.210×10^{-21}	2.498	33.601	6 0 6, A'	6 1 6, A''	ν_8
936.844	1.015×10^{-21}	2.368	24.091	5 0 5, A''	5 1 5, A'	ν_8
979.163	1.403×10^{-22}	0.841	38.475	3 3 1, A''	2 2 1, A'	ν_4
979.169	1.403×10^{-22}	0.842	38.475	3 3 0, A'	2 2 0, A''	ν_4
985.491	1.002×10^{-22}	0.563	22.502	3 2 2, A'	2 1 2, A''	ν_4
985.944	1.077×10^{-22}	0.606	22.534	3 2 1, A''	2 1 1, A'	ν_4
991.686	1.237×10^{-22}	0.674	13.409	3 1 2, A'	2 0 2, A''	ν_4
997.130	1.001×10^{-22}	0.880	4.733	1 1 1, A''	1 0 1, A'	ν_4
997.285	1.686×10^{-22}	0.903	7.810	2 1 2, A'	2 0 2, A''	ν_4
1003.137	1.710×10^{-22}	0.913	4.856	2 0 2, A'	2 1 2, A''	ν_4
1003.296	1.016×10^{-22}	0.891	1.621	1 0 1, A''	1 1 1, A'	ν_4
1006.857	1.030×10^{-22}	0.545	1.621	1 0 1, A''	2 1 1, A'	ν_4
1008.717	1.342×10^{-22}	0.518	4.856	2 0 2, A'	3 1 2, A''	ν_4

17 T. Millar, *Plasma Sources Science and Technology*, 2015, **24**, 043001.
18 T. Coplen, W. Brand, M. Gehre, M. Gröning, H. Meijer, B. Toman and R. Verkouteren, *Anal. Chem.*, 2006, **78**, 2439–2441.
19 H. Feuchtgruber, E. Lellouch, G. Orton, T. De Graauw, B. Vandenbussche, B. Swinyard, R. Moreno, C. Jarchow, F. Billebaud, T. Cavalié, S. Sidher and P. Hartogh, *A&A.*, 2013, **551**, A126.
20 A. Nikitin, J. Champion, V. Tyuterev and L. Brown, *J.Mol.Spectrosc.*, 1997, **184**, 120–128.
21 A. Nikitin, J. Champion, V. Tyuterev, L. Brown, G. Mellau and M. Lock, *J. Mol.Struct.*, 2000, **517-518**, 1–24.
22 A. Nikitin, L. Brown, L. Féjard, J. Champion and V. Tyuterev, *J.Mol.Spectrosc.*, 2002, **216**, 225–251.
23 M. Rey, A. V. Nikitin and V. G. Tyuterev, *J. Chem. Phys.*, 2014, **141**, 044316.
24 M. Rey, A. V. Nikitin and V. G. Tyuterev, *J. Phys. Chem. A*, 2015, **119**, 4763–4779.
25 M. Rey, A. V. Nikitin and V. G. Tyuterev, *J. Mol. Spectrosc.*, 2013, **291**, 85–97.
26 M. Rey, A. V. Nikitin and V. G. Tyuterev, *Phys. Chem. Chem. Phys.*, 2013, **15**, 10049–10061.
27 D. Viglaska, M. Rey, T. Delahaye and A. Nikitin, *J. Quant. Spectrosc. Radiat. Transf.*, 2019, **230**, 142–154.
28 D. Viglaska, M. Rey, A. Nikitin and V. Tyuterev, *J. Chem. Phys.*, 2019, **150**, 194303.
29 M. Rey, A. Nikitin, Y. Babikov and V. Tyuterev, *J.Mol.Spectrosc.*, 2016, **327**, 138–158.
30 T. Delahaye, A. Nikitin, M. Rey, P. Szalay and V. Tyuterev, *J.Chem.Phys.*, 2014, **141**, 104301.
31 T. Delahaye, A. Nikitin, M. Rey, P. Szalay and V. Tyuterev, *Chem. Phys. Letters*, 2015, **639**, 275–282.
32 M. Rey, T. Delahaye, A. Nikitin and V. Tyuterev, *A&A*, 2016, **594**, A47.
33 B. Mant, A. Yachmenev, J. Tennyson and S. Yurchenko, *Mon. Not. R. Astron. Soc.*, 2018, **478**, 3220–3232.

Table 10 Selected strong transitions for $^{13}CHD^{12}CH_2$ computed at $T = 296$ K. A is the Einstein coefficient (in 1/s) and E_{low} is the lower state energy. "l" and "u" stand for lower and upper states.

$\tilde{\nu}$(cm^{-1})	I(cm/mol)	A(1/s)	E_{low}(cm^{-1})	$(JK_aK_c,C)^l$	$(JK_aK_c,C)^u$	Band
797.768	1.047×10^{-21}	1.363	58.572	8 1 8, A'	8 0 8,A''	ν_7
798.096	1.140×10^{-21}	1.421	72.332	9 1 9, A''	9 0 9,A'	ν_7
798.386	1.210×10^{-21}	1.471	87.588	10 1 10, A'	10 0 10,A''	ν_7
798.638	1.255×10^{-21}	1.512	104.333	11 1 11, A''	11 0 11,A'	ν_7
798.856	1.274×10^{-21}	1.544	122.562	12 1 12, A'	12 0 12,A''	ν_7
799.047	1.270×10^{-21}	1.569	142.268	13 1 13, A''	13 0 13,A'	ν_7
799.215	1.245×10^{-21}	1.587	163.449	14 1 14, A'	14 0 14,A''	ν_7
799.370	1.199×10^{-21}	1.598	186.101	15 1 15, A''	15 0 15,A'	ν_7
799.519	1.136×10^{-21}	1.600	210.222	16 1 16, A'	16 0 16,A''	ν_7
799.560	1.274×10^{-21}	1.574	141.997	13 0 13, A''	13 1 13,A'	ν_7
799.607	1.248×10^{-21}	1.592	163.256	14 0 14, A'	14 1 14,A''	ν_7
799.624	1.278×10^{-21}	1.549	122.186	12 0 12, A'	12 1 12,A''	ν_7
799.663	1.049×10^{-21}	1.578	235.807	17 1 17, A''	17 0 17,A'	ν_7
799.701	1.141×10^{-21}	1.607	210.125	16 0 16, A'	16 1 16,A''	ν_7
799.794	1.216×10^{-21}	1.478	86.899	10 0 10, A'	10 1 10,A''	ν_7
896.237	4.617×10^{-22}	1.804	48.789	6 6 0, A'	5 5 0,A''	ν_8
903.224	4.610×10^{-22}	1.543	13.819	6 5 1, A''	5 4 1,A'	ν_8
910.086	4.406×10^{-22}	1.302	85.202	6 4 3, A''	5 3 3,A'	ν_8
911.737	4.409×10^{-22}	1.524	75.404	5 4 1, A''	4 3 1,A'	ν_8
913.382	4.437×10^{-22}	1.901	67.242	4 4 0, A'	3 3 0,A''	ν_8
916.734	4.031×10^{-22}	1.084	62.949	6 3 4, A'	5 2 4,A''	ν_8
918.427	3.907×10^{-22}	1.229	53.140	5 3 3, A''	4 2 3,A'	ν_8
986.044	1.567×10^{-22}	5.034	28.832	5 1 4, A'	4 0 4,A''	ν_4
986.836	1.005×10^{-22}	2.449	47.355	6 2 4, A'	6 1 6,A''	ν_4
987.574	1.017×10^{-22}	2.795	37.389	5 2 3, A''	5 1 5,A'	ν_4
988.130	1.430×10^{-22}	5.690	20.297	4 1 3, A''	3 0 3,A'	ν_4
989.867	1.246×10^{-22}	4.036	29.030	4 2 3, A''	4 1 3,A'	ν_4
990.111	1.225×10^{-22}	6.623	13.459	3 1 2, A'	2 0 2,A''	ν_4
990.253	1.569×10^{-22}	4.328	37.164	5 2 4, A'	5 1 4,A''	ν_4
990.707	1.878×10^{-22}	4.601	46.912	6 2 5, A''	6 1 5,A'	ν_4
995.746	1.670×10^{-22}	8.886	7.824	2 1 2, A'	2 0 2,A''	ν_4

34 L. Ng, T. Tan, L. Akasyah, A. Wong, D. Appadoo and D. McNaughton, *J. Mol. Spectrosc.*, 2017, **340**, 29–35.

35 L. Ng, T. Tan, A. Wong, D. Appadoo and D. McNaughton, *Mol. Phys.*, 2016, **114**, 2798–2807.

36 T. Tan and M. Gabona, *J. Mol. Spectrosc.*, 2012, **272**, 51–54.

37 T. Tan and G. Lebron, *J. Mol. Spectrosc.*, 2010, **261**, 87–90.

38 L. Ng, T. Tan and M. Gabona, *J. Mol. Spectrosc.*, 2015, **316**, 90–94.

39 M. Gabona and T. Tan, *J. Mol. Spectrosc.*, 2014, **299**, 31–34.

40 K. Goh, T. Tan, P. Ong and H. Teo, *Chem. Phys. Letters*, 2000, **325**, 584–588.

41 G. Lebron and T. Tan, *J. Mol. Spectrosc.*, 2012, **271**, 44–49.

42 O. Ulenikov, O. Gromova, E. Bekhtereva, Y. Aslapovskaya, A. Ziatkova, C. Sydow, C. Maul and S. Bauerecker, *J. Quant. Spectrosc. Radiat. Transfer*, 2016, **184**, 76–88.

43 O. Ulenikov, O. Gromova, E. Bekhtereva, K. Berezkin, E. Sklyarova, C. Maul, K.-H. Gericke and S. Bauerecker, *J. Quant. Spectrosc. Radiat. Transfer*, 2015, **161**, 180–196.

44 Y. A. Ba, C. Wenger, R. Surleau, V. Boudon, M. Rotger, L. Daumont, D. A. Bonhommeau, V. G. Tyuterev and M. L. Dubernet, *J. Quant. Spectrosc. Radiat. Transf.*, 2013, **130**, 62–68.

45 I. Gordon, L. Rothman, C. Hill, R. Kochanov, Y. Tan, Bernath *et al.*, *J. Quant. Spectrosc. Radiat. Transfer*, 2017, **203**, 3–69.

46 N. Jacquinet-Husson, R. Armante, N. Scott, A. Chédin, Crépeau *et al.*, *J.Mol.Spectrosc.*, 2016, **327**, 31–72.

47 C. Courtoy and M. de Hemptine, *Ann. Soc. Sci. Bruxelles, Ser.I.*, 1953, **67**, 285–295.
48 C. Courtoy and M. de Hemptine, *Ann. Soc. Sci. Bruxelles, Ser.I.*, 1953, **67**, 296–308.
49 J. Duncan, D. McKean and P. Mallinson, *J. Mol. Spectrosc.*, 1973, **45**, 221–246.
50 J. Duncan, A. Ferguson and S. Goodlad, *Spectroc. Acta A : Mol. Spectrosc.*, 1993, **49**, 149–160.
51 J. Martin, T. Lee, P. Taylor and J.-P. Francois, *J. Chem. Phys.*, 1995, **103**, 2589–2602.
52 T. Tan and G. Lebron, *J. Mol. Spectrosc.*, 2011, **269**, 109–112.
53 L. Ng, T. Tan, M. Gabona, P. Godfrey and D. McNaughton, *J. Mol. Spectrosc.*, 2015, **316**, 79–83.
54 L. Ng, T. Tan and A. Chia, *J. Mol. Spectrosc.*, 2018, **344**, 27–33.
55 J. Duncan and A. Ferguson, *J. Chem. Phys.*, 1988, **89**, 4216–4226.
56 J. Duncan, *Mol. Phys.*, 1994, **83**, 159–169.
57 J. Duncan, E. Hamilton, A. Fayt, D. Van Lerberghe and F. Hegelund, *Mol. Phys.*, 1981, **43**, 737–752.
58 J. Harper and J. Duncan, *Mol. Phys.*, 1982, **46**, 139–149.
59 J. Harper, A. Morrisson and J. Duncan, *Chem. Phys. Lett.*, 1981, **83**, 32–36.
60 A.-K. Mose, F. Hegelund and F. Nicolaisen, *J. Mol. Spectrosc.*, 1989, **137**, 286–295.
61 F. Mompeán, R. Escribano, S. Montero, J. Bendtsen and R. Butcher, *J. Mol. Spectrosc.*, 1986, **116**, 48–57.
62 T. Tan, K. Goh, P. Ong and H. Teo, *J. Mol. Spectrosc.*, 2000, **202**, 249–252.
63 K. Goh, T. Tan, P. Ong and H. Teo, *Mol. Phys.*, 2002, **98**, 583–587.
64 T. Tan, K. Goh, P. Ong and H. Teo, *Chem. Phys. Letters*, 1999, **315**, 82–86.
65 T. Tan, M. Gabona, D. Appadoo, P. Godfrey and D. McNaughton, *J. Mol. Spectrosc.*, 2014, **303**, 42–45.
66 M. Rey, I. Chizhmakova, A. Nikitin and V. Tyuterev, *Phys. Chem. Chem. Phys.*, 2018, **20**, 21008–21033.
67 D. Viglaska, M. Rey, A. Nikitin and V. Tyuterev, *J. Chem. Phys*, 2018, **149**, 174305.
68 M.Rey, A.V.Nikitin and V.G.Tyuterev, *J. Chem. Phys.*, 2012, **136**, 244106.
69 M. Rey, A. V. Nikitin and V. G. Tyuterev, *J. Quant. Spectrosc. Radiat. Transf.*, 2015, **164**, 207–220.
70 J. Watson, *Mol.Phys.*, 1968, **15**, 479–490.
71 N. R. Zare, *Angular Momentum: Understanding Spatial Aspects in Chemistry and Physics*, Wiley, 1991.
72 P. R. Bunker and P. Jensen, *Molecular Symmetry and Spectroscopy*, NRC-CNRC, Ottawa, 1998.
73 P. Bunker and P. Jensen, *Fundamentals of molecular symmetry*, IOP Publishing, London, 2005.
74 T. Tan, M. Gabona and G. Lebron, *J. Mol. Spectrosc.*, 2011, **266**, 113–115.

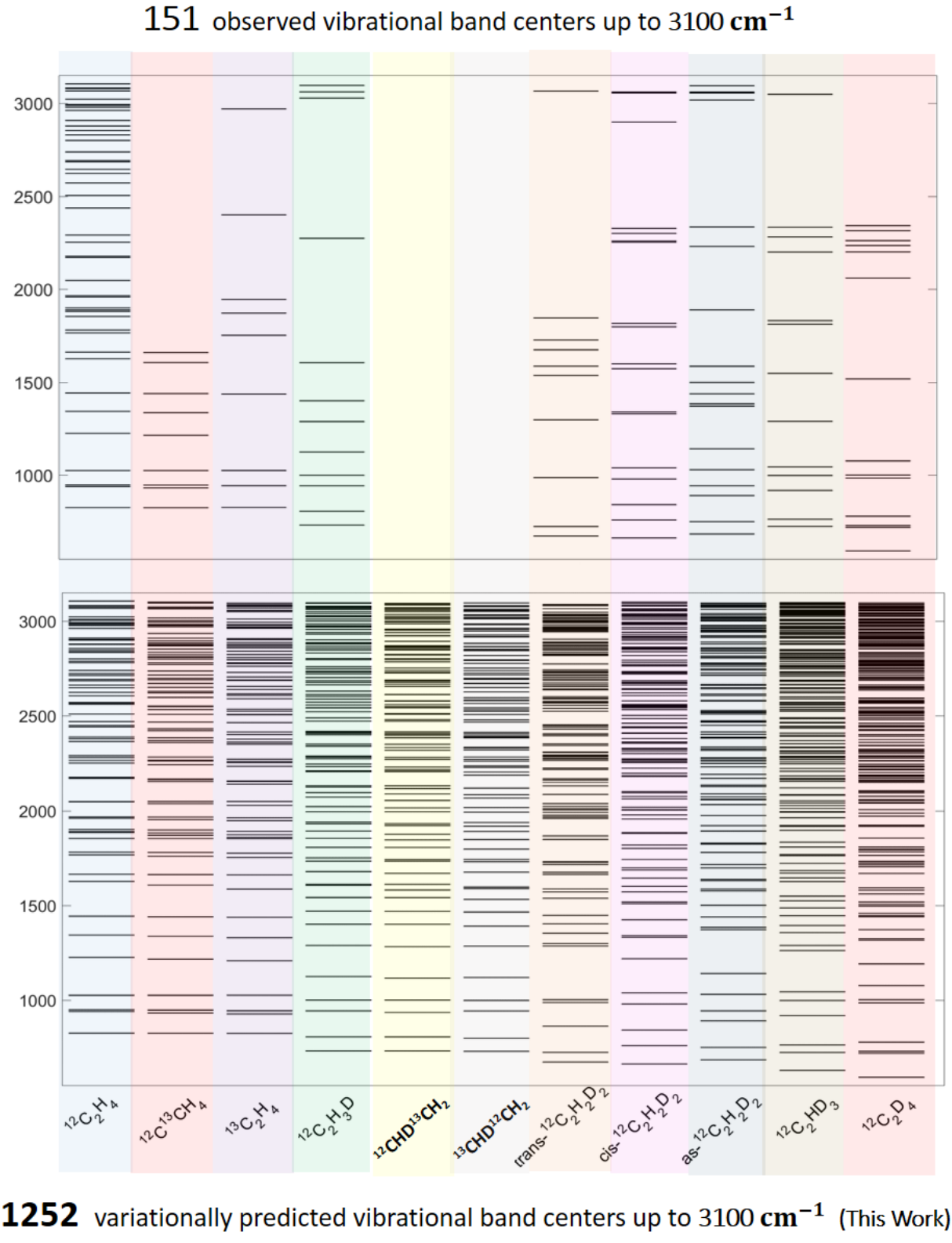

Fig. 1 Observed vibrational band centers determined by empirical analysis (upper panel) and variationally predicted energy levels for 11 ethylene isotopologues (lower panel) in the range ≤ 3100 cm^{-1}.

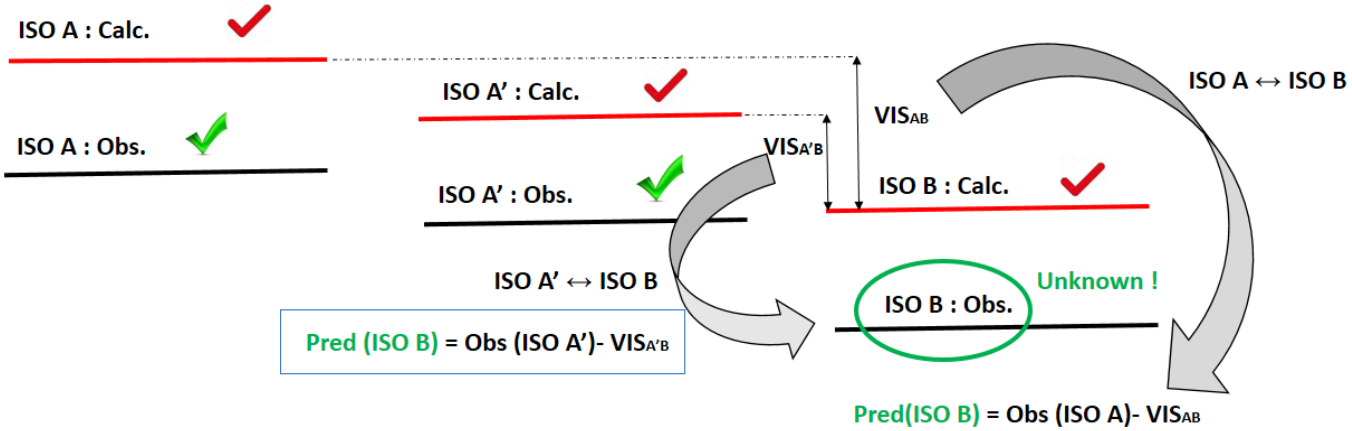

Fig. 2 Schematic representation of vibrational isotopic shift method based on the ”mother” (IsoA) and ”pseudo mother” (IsoA') molecules.

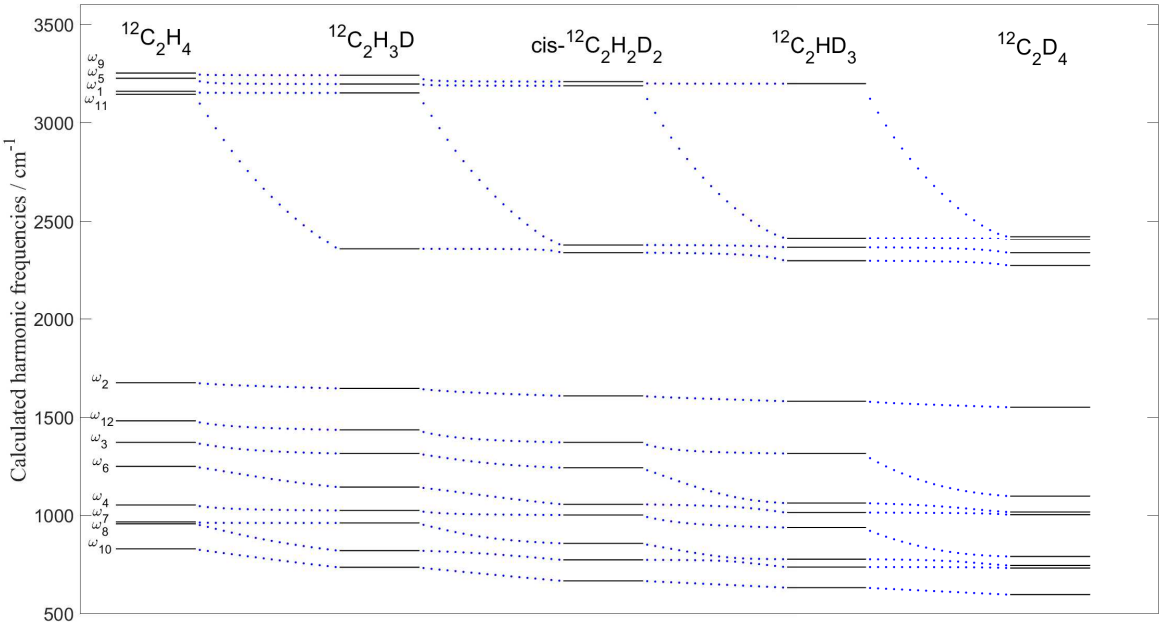

Fig. 3 Correlation diagram for harmonic frequencies for five ethylene isotopologues from successive quasi-continuous H → D substitutions from $^{12}C_2H_4$ to $^{12}C_2D_4$ (see text).

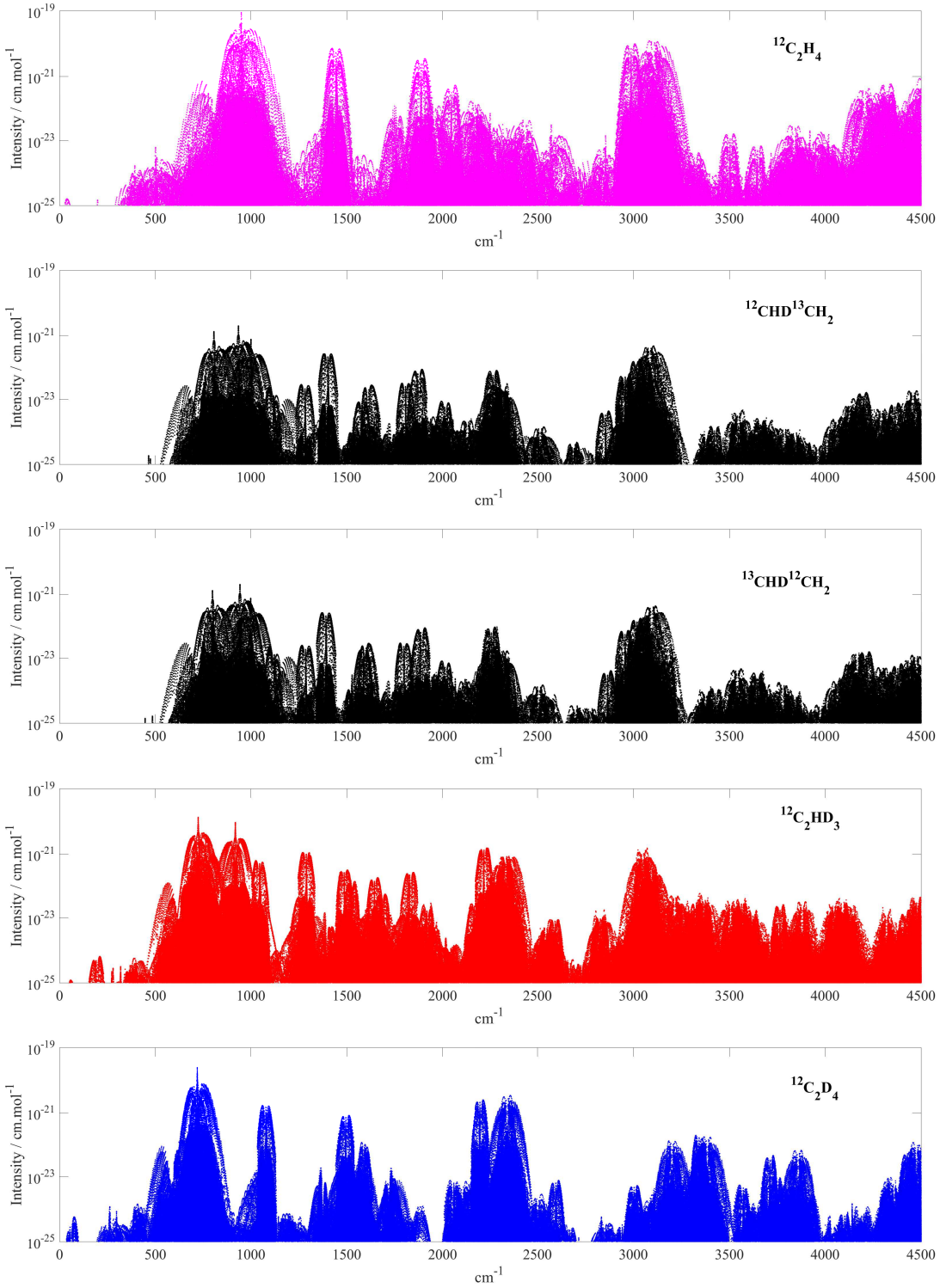

Fig. 4 Overview spectrum of $^{12}C_2H_4$, $^{12}CHD^{13}CH_2$,$^{13}CHD^{12}CH_2$, $^{12}C_2HD_3$ and $^{12}C_2D_4$ from calculation at 296 K in log scale using the *ab initio* PES and DMS of Refs.[31],[30].

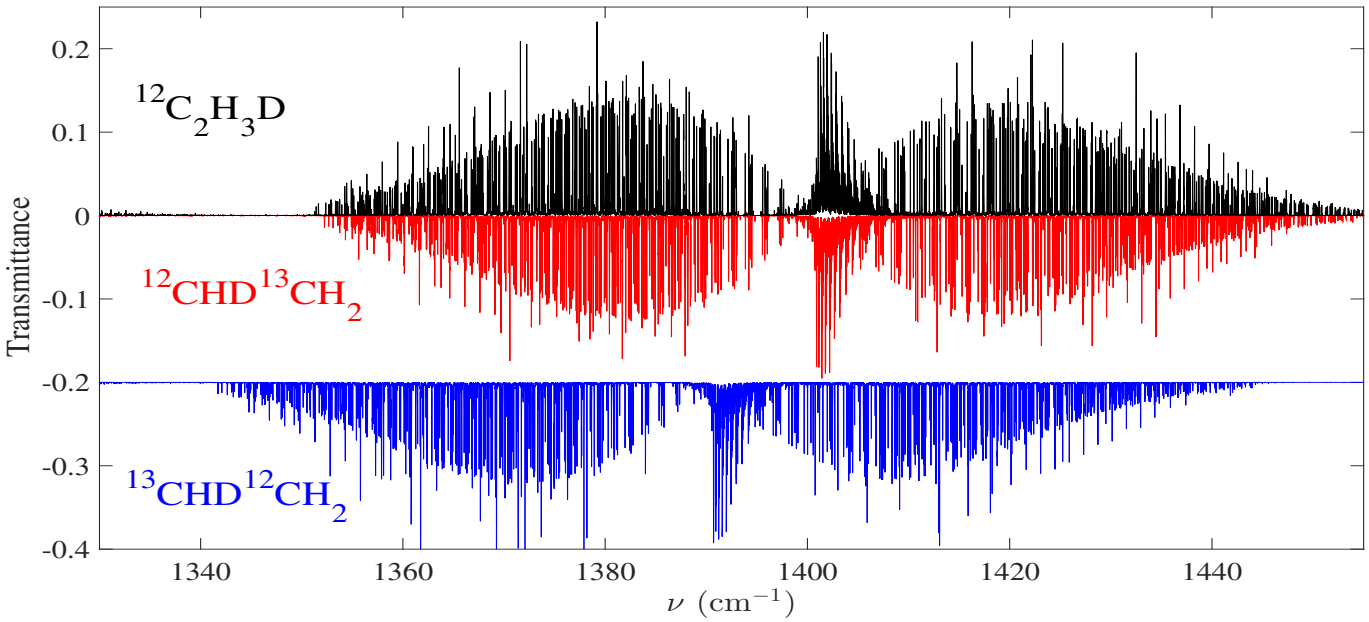

Fig. 5 Comparison between $^{12}C_2H_3D$ and $^{12}CHD^{13}CH_2$ and $^{13}CHD^{12}CH_2$ simulated spectra in the region 1330−1480 cm^{-1}.

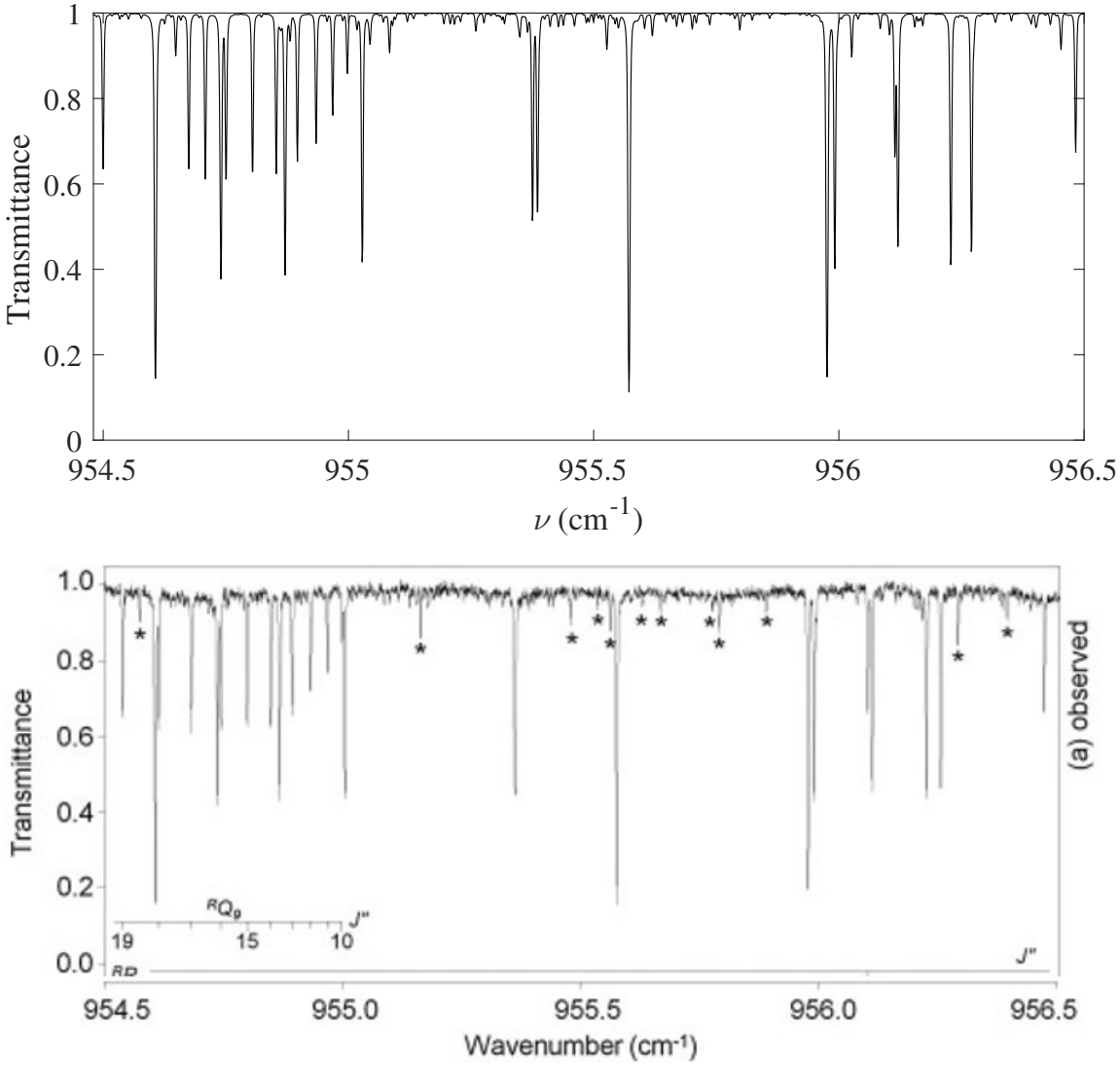

Fig. 6 Detailed portion of the ν_8 band of $^{12}C_2HD_3$ obtained by variational calculations (this work) (top panel) compared to experiment (bottom panel) taken from Fig. 3 of Ref.[34]

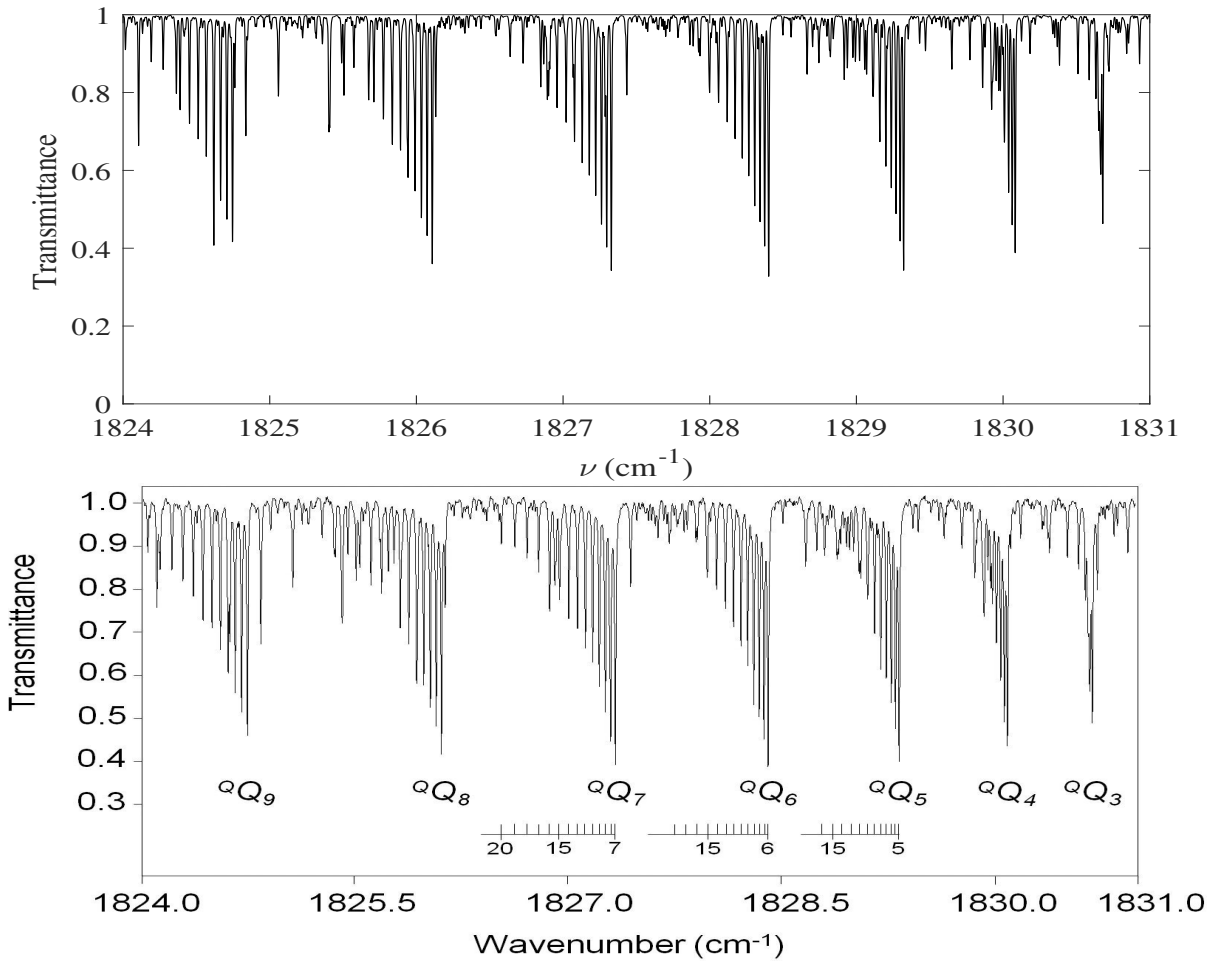

Fig. 7 Detailed portion of the $2\nu_8$ band of $^{12}C_2HD_3$ obtained by variational calculations (this work) (top panel) compared to experiment (bottom panel) taken from Fig. 2 of Ref.[54]

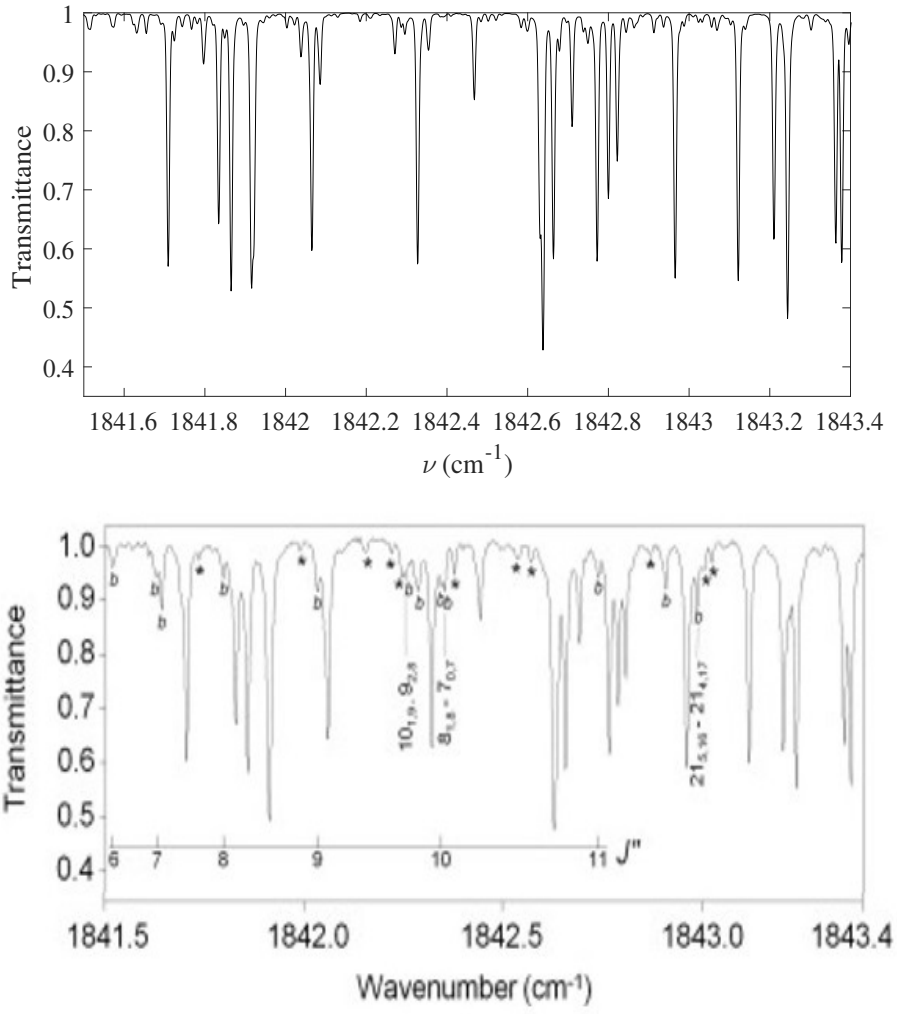

Fig. 8 Detailed portion of the R branch of the $2\nu_8$ band of $^{12}C_2HD_3$ obtained from variational calculations (this work) (top panel) compared to experiment (bottom panel) taken from Fig. 3 of Ref.[54]

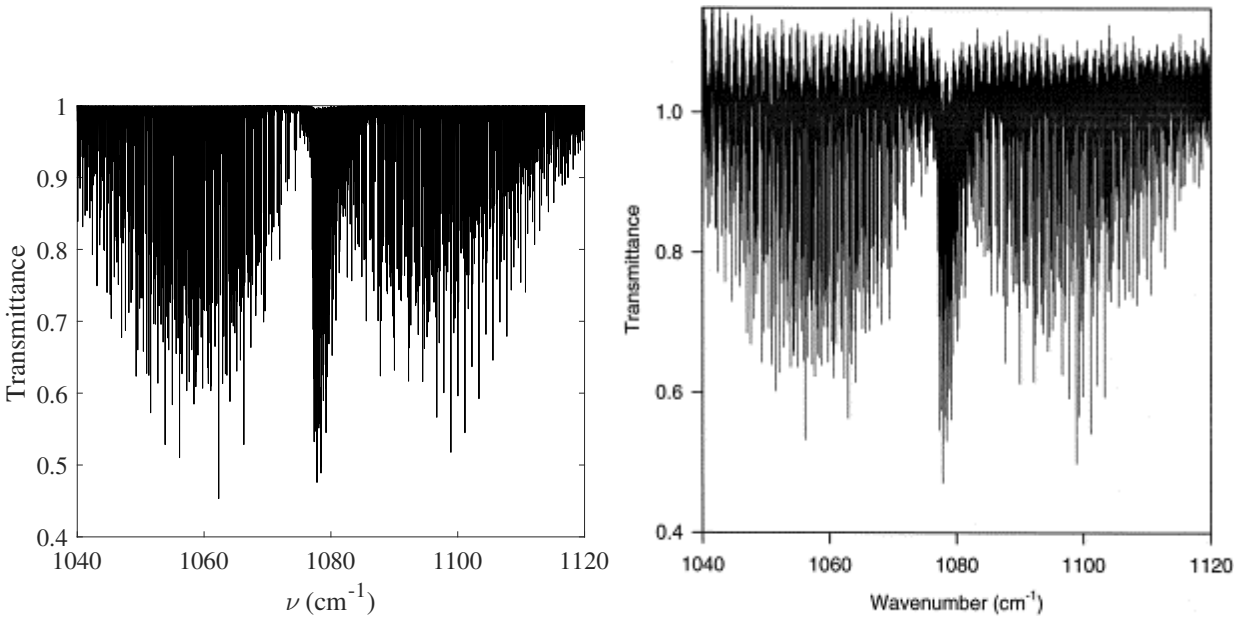

Fig. 9 Survey spectrum of the ν_{12} band of $^{12}C_2D_4$ obtained by variational calculations (this work) (left) compared to experiment (right) taken from Fig. 1 of Ref.[64]

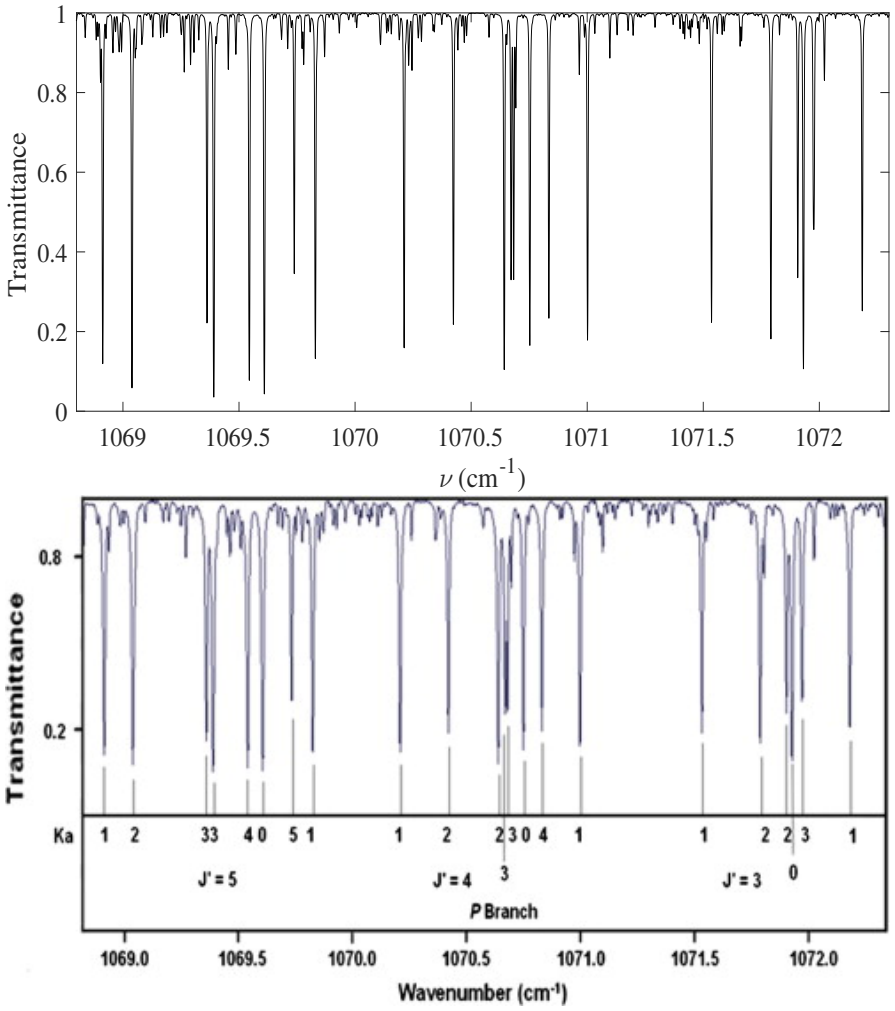

Fig. 10 Detailed portion of the P branch of the ν_{12} band of $^{12}C_2D_4$ obtained by variational calculations (this work) (top panel) compared to experiment (bottom panel) taken from Fig. 1 of Ref. [74]

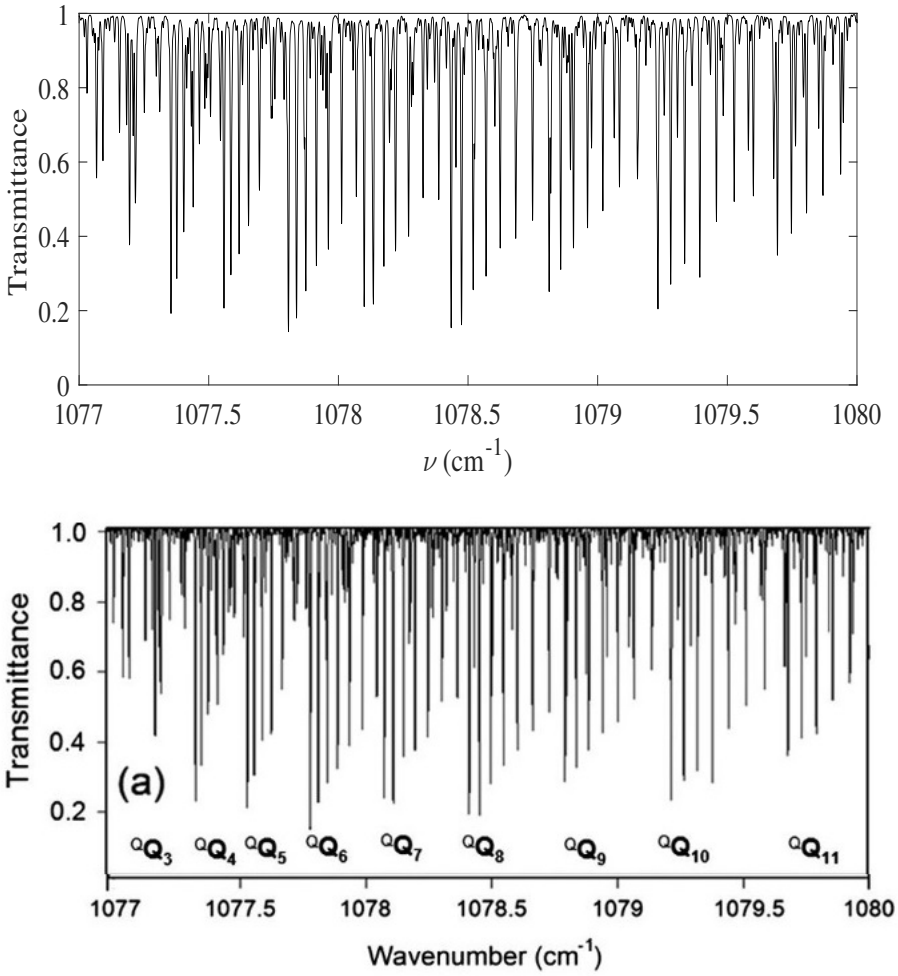

Fig. 11 Portion spectrum of the ν_{12} band of $^{12}C_2D_4$ in the region of 1078 cm^{-1} obtained by variational calculations (this work) (top panel) compared to experiment (bottom panel) taken from Fig. 2 of Ref. [65]

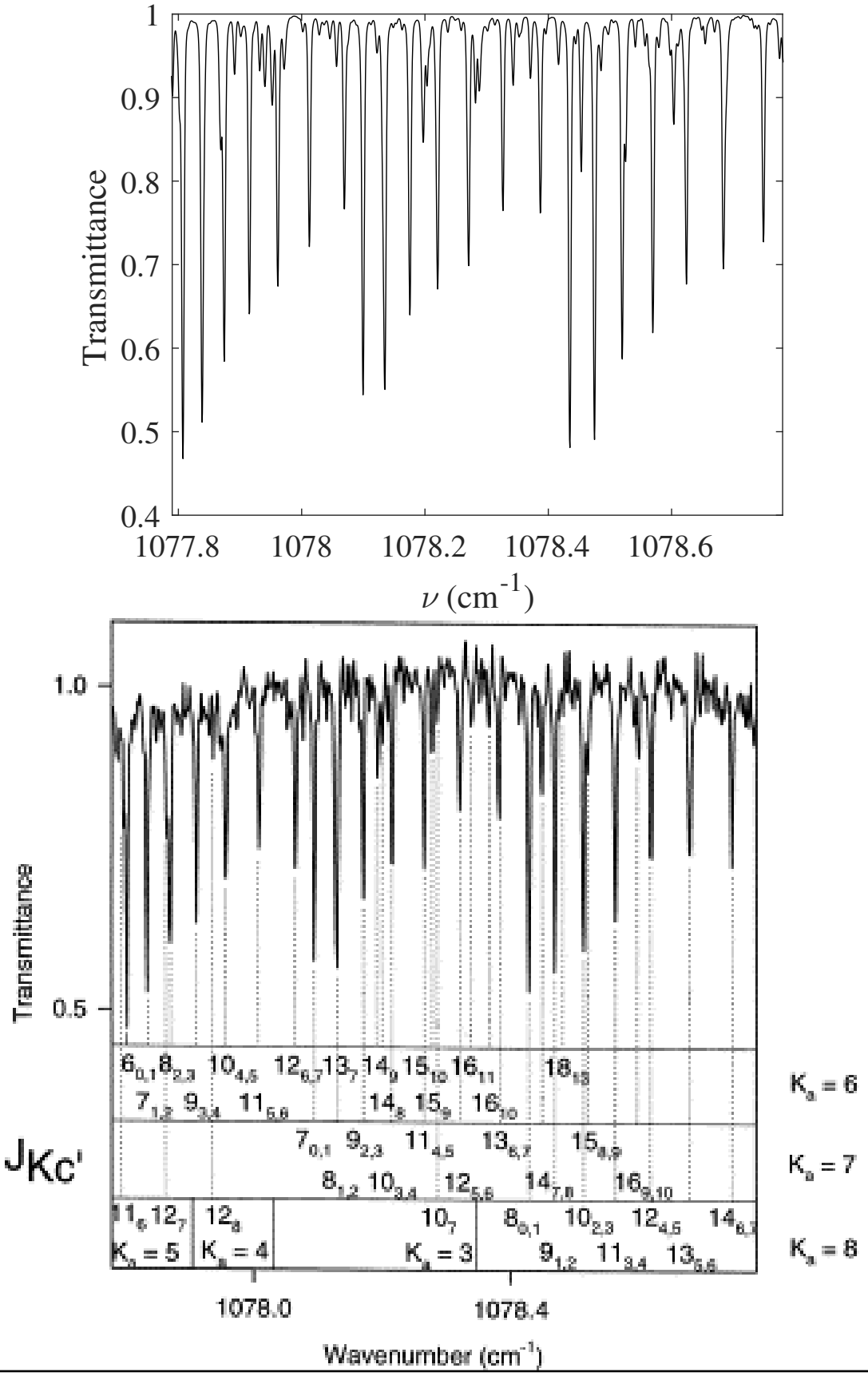

Fig. 12 Detailed portion of the Q branch of the ν_{12} band of $^{12}C_2D_4$ obtained by variational calculations (this work) (top panel) compared to experiment (bottom panel) taken from Fig. 2 of Ref. [64]

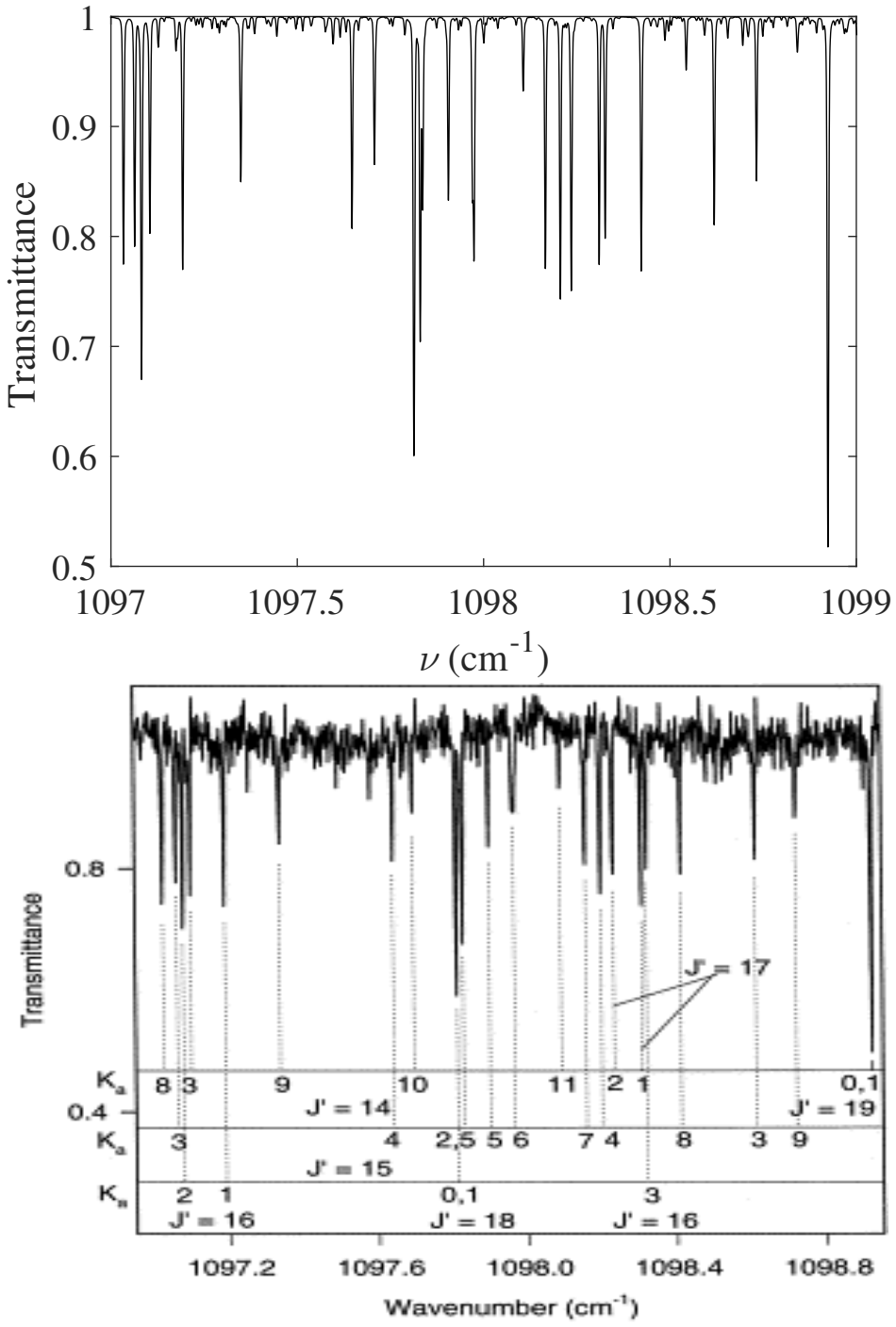

Fig. 13 Detailed portion of the *R* branch of the ν_{12} band of $^{12}C_2D_4$ obtained by variational calculations (this work) (top panel) compared to experiment (bottom panel) taken from Fig. 4 of Ref. [64]

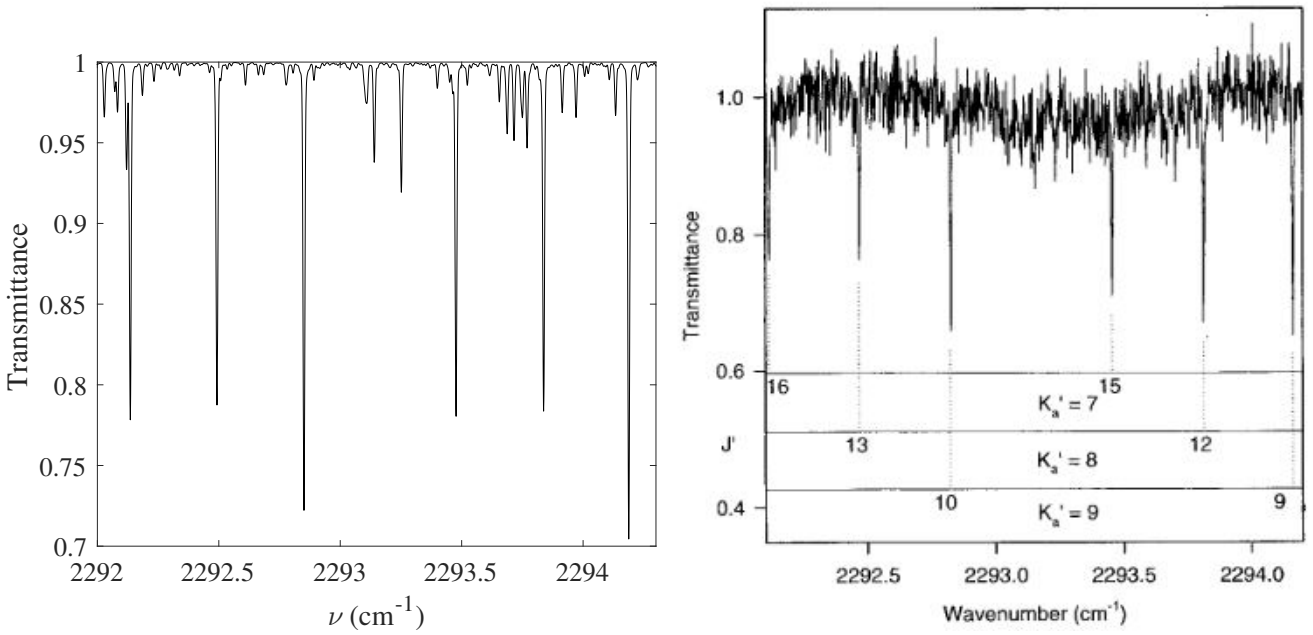

Fig. 14 Detailed portion of the P branch of ν_9 band of $^{12}C_2D_4$ obtained by variational calculations (this work) (left) compared to experiment (right) taken from Fig. 2 of Ref.[62]

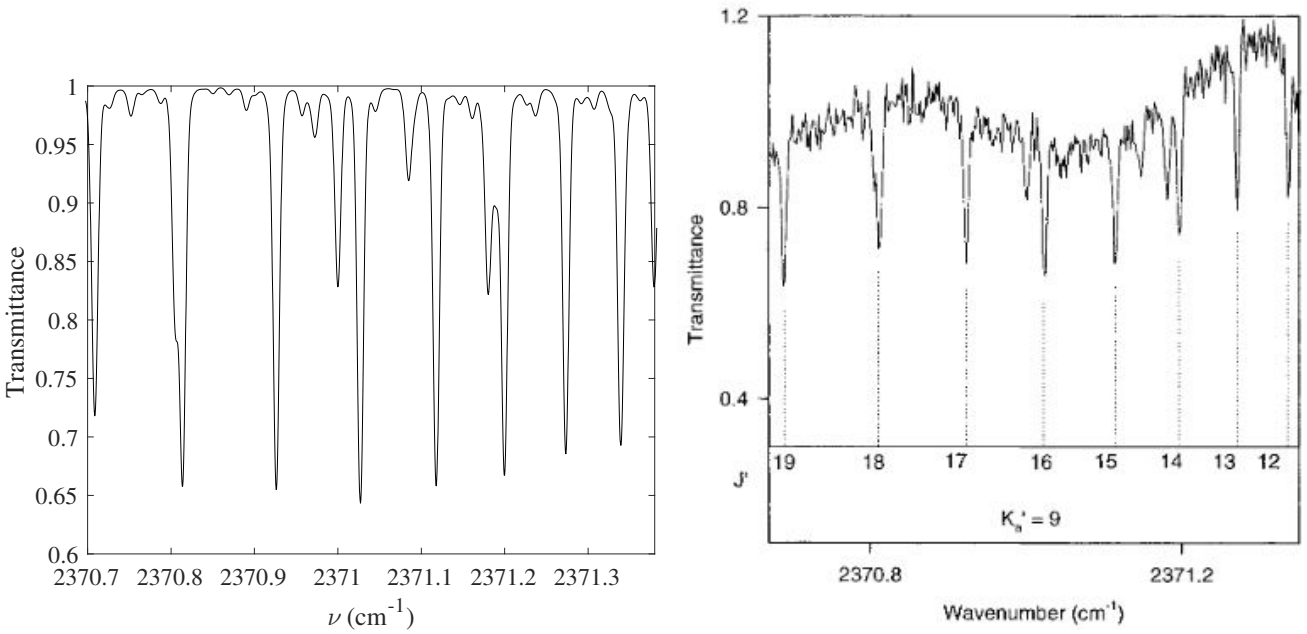

Fig. 15 Detailed portion of the Q branch of ν_9 band of $^{12}C_2D_4$ obtained by variational calculations (this work) (left) compared to experiment (right) taken from Fig. 4 of Ref.[62]